Research Square

Preprints are preliminary reports that have not undergone peer review.
They should not be considered conclusive, used to inform clinical practice,
or referenced by the media as validated information.

Hybrid Geothermal System Characterization of the Paipa–Iza Complex (Colombia) Using Analogue Comparison and Maturity Index Analysis

Arian Sarmiento-Orjuela
arian.sarmiento@uamerica.edu.co

Fundación Universidad de America

Arnul Paz
Fundación Universidad de America

Diego Acuña
Fundación Universidad de America

Harold Aldana
Fundación Universidad de America

Juan Diego Valencia
Fundación Universidad de America

Research Article

Keywords: Paipa–Iza Geothermal System, Hybrid geothermal systems, Exploration risk reduction, Geothermal Maturity Index (GMI)

Posted Date: August 28th, 2026

DOI: https://doi.org/10.21203/rs.3.rs-10730524/v1

License: This work is licensed under a Creative Commons Attribution 4.0 International License. Read Full License

Additional Declarations: No competing interests reported.

Abstract

The Paipa–Iza Geothermal System (PIGS), located in the Eastern Cordillera of Colombia, represents a promising but structurally uncharacterized resource within the Northern Andes. This study applies an analogue-based methodology, comparing the system against six representative global geothermal fields (Cerro Prieto, the German Molasse Basin, the North German Basin, Aachen, the Pannonian Basin, and Central Tuscany), to characterize its reservoir architecture and fluid circulation mechanisms. The synthesis of geological, geochemical, and geophysical evidence indicates that Paipa–Iza is a hybrid geothermal system: a structurally controlled sedimentary reservoir, hosted along the Une Formation and Guadalupe Group, that is thermally sustained by Miocene–Pleistocene felsic intrusions with a possible subsidiary radiogenic contribution. To quantify development potential independently of reservoir temperature, this study introduces the Geothermal Maturity Index (GMI), a composite indicator integrating project status, infrastructure, final resource use, and technical characterization. Paipa–Iza achieves a GMI of 0.3625 (Monte Carlo median = 0.353; 95% uncertainty interval: 0.198–0.487; n = 50,000 realizations), representing low maturity with high exploration potential, although uncertainties regarding heat-source partitioning and hydraulic connectivity persist. Cross-validation against a database-derived benchmark of 229 globally scored geothermal systems, together with a structured, SGC-reviewed knowledge-gap diagnostic, independently confirms this low-maturity classification and identifies subsurface geophysical characterization, 3D conceptual modeling, and exploratory drilling as the principal barriers to advancing the system. These findings demonstrate the critical role of structural control and analogue-based frameworks in de-risking exploration within hybrid geothermal systems of the Northern Andes.

1. Introduction

The global energy transition has elevated geothermal energy as a strategic resource, owing to its capacity to deliver firm, dispatchable baseload power with minimal surface footprint and low lifecycle emissions (Snyder, 2019). Unlike intermittent renewables, geothermal systems provide high-availability thermal and electrical output, making them a critical component of decarbonization strategies in volcanic arcs, sedimentary basins, and structurally complex orogens alike (Ito and Ruiz, 2017). In Latin America, however, geothermal development remains heavily concentrated in the volcanic provinces of the Pacific Rim — Mexico, Central America, and the Chilean Andes — while the extensive sedimentary and hybrid systems of the Northern and Eastern Andes remain largely underexplored and poorly characterized (Ito and Ruiz, 2017). This disparity reflects not only geological uncertainty, but also the absence of systematic, reproducible assessment frameworks that can guide exploration in data-limited environments.

Within this context, the Paipa–Iza geothermal complex (Eastern Cordillera, Colombia) represents one of the most promising and yet most poorly constrained geothermal prospects in South America. The system is situated within a Cenozoic compressional basin shaped by the inversion of Cretaceous extensional structures, where a thick sedimentary sequence — dominated by the Une and Guadalupe formations — is intruded by Miocene–Pleistocene felsic magmas that constitute the primary heat source (OECD, 2008; Alfaro et al., 2010). A hierarchical network of regional faults (Boyacá, Soapaga, Paipa–Iza, Cerro Plateado, among others) segments the basement and cover, controls permeability anisotropy, and enables vertical hydraulic connectivity for deep fluid circulation (OECD, 2008; Alfaro et al., 2010). Surface manifestations — thermal springs, hydrothermal alteration zones, and diffuse degassing — confirm active fluid circulation at shallow depths, while reported temperatures of 65–90°C constrain the system to a low-to-medium enthalpy range (Dijkshoorn et al., 2013). Additionally, geochemical and mineralogical analyses of drill cores have documented significant enrichments in U, Th, and K within intensely altered intrusions at the El Durazno sector, suggesting a non-negligible radiogenic heat contribution that distinguishes Paipa–Iza from purely sedimentary geothermal systems (Alfaro-Valero et al., 2019).

Despite this geological complexity, the characterization of Paipa–Iza remains incomplete at every critical dimension of geothermal resource assessment. The partitioning of heat between the magmatic intrusions and the possible radiogenic component is unresolved. The architecture of the sedimentary reservoir — its lateral continuity, effective permeability, and structural compartmentalization — has not been quantified at the engineering scale. The connectivity between the deep faulted basement and the shallow hydrothermal circulation remains inferential, based on surface geophysics (magnetotellurics, gravimetry, magnetometry) rather than on direct subsurface data (Alfaro et al., 2010; Gilbert, 2019; Beltrán, 2015). No production well has been drilled, and no thermal or hydrogeological model has been calibrated against downhole measurements. The system therefore occupies a critical stage in geothermal exploration: conceptually interpreted, geophysically imaged, but insufficiently characterized to support investment decisions or development design.

This knowledge gap is not unique to Colombia. Across the Northern Andes, emerging geothermal systems in sedimentary or hybrid settings face a common methodological challenge: the absence of locally drilled analogues makes it difficult to bound resource estimates, identify productive structural targets, or anticipate reservoir behavior under exploitation. In this context, analogue-based approaches offer a proven strategy for reducing conceptual uncertainty by transferring interpretive criteria, property ranges, and development lessons from well-characterized fields to data-limited environments (Yin and Campbell, 2018). Such frameworks are widely applied in both the petroleum and geothermal industries, and have been formalized in international assessment guidelines (Ito and Ruiz, 2017). However, their application to Andean hybrid systems — where sedimentary reservoirs coexist with magmatic and possible radiogenic heat sources under compressional structural regimes — has not been systematically pursued in the peer-reviewed literature.

A second methodological gap compounds this problem. Current tools for benchmarking geothermal prospects tend to focus on temperature and enthalpy classification alone, treating all medium-enthalpy systems as comparable regardless of their development stage, infrastructure maturity, or level of subsurface characterization (Ito and Ruiz, 2017). This conflation prevents meaningful comparison between, for example, a system with decades of operational data and reinjection infrastructure and one at the surface-reconnaissance stage. A composite indicator that integrates multiple dimensions of maturity — project status, installed infrastructure, resource utilization, and technical characterization depth — would allow for a more nuanced and actionable positioning of emerging prospects relative to global benchmarks.

This methodological gap must be situated relative to existing staged and multi-axis geothermal classification frameworks. The United Nations Framework Classification for Resources (UNFC), piloted on real-world geothermal projects across fourteen countries, evaluates a resource along three independent axes — economic viability, project maturity, and geological confidence — and assigns a composite alphanumeric code rather than a single continuous score (Beardsmore et al., 2021). Industry-oriented staged models, including the four-phase scheme of the Geothermal Energy Association (GEA), the equivalent classification used by SNL Financial for project finance, and the five-stage framework maintained by Open Energy Information (Unconfirmed, Early Exploration, Advanced Exploration, Advanced Resource Development, and Under Construction), describe qualitative development milestones but do not integrate infrastructure type, resource utilization, or the breadth of technical characterization into a single quantitative index (OpenEI, 2018). Moeck (2014) instead classifies systems genetically, by heat source and reservoir architecture, which is directly informative for interpreting Paipa–Iza's hybrid magmatic–radiogenic setting (Section 3.1.1) but addresses geological typology rather than development maturity. None of these frameworks, individually, yields a continuously scored, reproducible index computable from the coarse, publicly available data typical of early-stage prospects. The GMI introduced below is accordingly proposed as a complementary quantitative layer — compatible with, rather than a substitute for, the qualitative staging vocabulary of UNFC, GEA, SNL, and OpenEI — designed to enable transparent benchmarking across large, heterogeneous system inventories, including the 229-system global dataset introduced in Section 2.1.1 and applied in Section 3.9.

This study addresses both gaps through a systematic, analogue-based characterization of the Paipa–Iza Geothermal System (PIGS), combined with the development and application of a novel Geothermal Maturity Index (GMI). Six international analogues were selected through structured screening criteria, including geological similarity, enthalpy range, tectonic setting, and data availability: Cerro Prieto (Mexico), the German Molasse Basin, the North German Basin, Aachen (Germany), the Pannonian Basin (Hungary), and Central Tuscany (Larderello–Travale and Monte Amiata, Italy). These systems collectively span the full spectrum from low-enthalpy sedimentary aquifers to high-enthalpy vapor-dominated volcanic fields, enabling multidimensional comparison of heat sources, reservoir architectures, permeability controls, and development trajectories. The GMI was constructed following established composite indicator methodology (OECD, 2008), incorporating four normalized dimensions — project development status, type of geothermal infrastructure, final resource use, and level of technical characterization — and validated through sensitivity analysis of alternative weighting scenarios. The resulting index is further validated through a 50,000-realization Monte Carlo uncertainty analysis and cross-checked against an independently scored, 229-system global benchmark (Section 3.9), providing a level of external validation rarely available for composite geothermal maturity indicators.

The specific objectives of this study are: (1) to characterize the geological, structural, thermal, and hydrothermal architecture of Paipa–Iza through a systematic synthesis of published data; (2) to compare PIGS against six international analogues using a standardized multidimensional framework; (3) to introduce and apply the GMI as a reproducible composite indicator for benchmarking geothermal system maturity; and (4) to identify transferable exploration and development lessons applicable to Paipa–Iza and, more broadly, to emerging hybrid geothermal systems in the Northern Andes. By integrating analogue transfer with quantitative maturity assessment, this work aims to provide a structured, evidence-based framework for reducing exploration risk and supporting strategic decision-making in one of South America's most promising but underexplored geothermal provinces.

2. Materials and Methods

2.1 Research Design and Literature Review Strategy

The methodology of this study adopted a qualitative, comparative, and exploratory-descriptive research design to identify transferable technical concepts between global geothermal systems and the Paipa–Iza Geothermal System (PIGS). The comparative approach follows transverse research methodologies (Yin and Campbell, 2018), enabling a structured and multidimensional evaluation across diverse geological contexts.

The initial stage focused on an exhaustive literature review comprising approximately 500 scientific documents, including peer-reviewed journal articles, conference proceedings, technical reports, and institutional publications. Comprehensive bibliographic searches were conducted using Scopus, Web of Science, ScienceDirect, and Google Scholar, and were further supplemented by institutional repositories from the International Geothermal Association (IGA), the International Renewable Energy Agency (IRENA), the United States Geological Survey (USGS), and the World Geothermal Congress.

Search strategies were specifically tailored to identify studies addressing low-, medium-, and high-enthalpy geothermal systems, hydrothermal reservoirs, geological analogues, volcanic and non-volcanic settings, direct-use applications, and projects in advanced exploration or production stages. Consequently, selection criteria prioritized studies providing verifiable technical data regarding:

- Geological and tectonic settings,
- Reservoir temperature and depth,
- Geothermal fluid type and hydrothermal regimes,
- Reservoir lithology and caprock characteristics,
- Surface manifestations, and
- Current development stage.

These parameters are widely recognized as standard descriptors within geothermal resource assessment frameworks (Ito and Ruiz, 2017). The macro-dataset generated from this comprehensive screening—encompassing geographical distribution, enthalpy classifications, geothermal system types, and temperature-depth relationships—is statistically synthesized in Fig. 1.

2.1.1 Extended Global Benchmark Dataset and Bibliometric Synthesis

To support the analogue comparison described above and to provide an independent, database-derived benchmark for the GMI (Section 2.3), the approximately 500 documents identified during the literature review were formally coded into a structured bibliometric matrix comprising 501 records spanning 1978–2026, drawn from Scopus, Web of Science, ScienceDirect, SpringerLink, and the proceedings of the World Geothermal Congress and the Stanford Geothermal Workshop. Each record was classified by continent, country, publication type, and by the presence, partial presence, or absence of coverage across seven technical dimensions: modeling, geology, geophysics, geochemistry, drilling and production, theoretical context, and simulation/validation. This synthesis shows that theoretical context is addressed, at least partially, in 98.6% of the reviewed literature, followed by geology (76.0%) and modeling (59.7%), while geophysics (39.3%), geochemistry (44.5%), and drilling/production (31.1%) are comparatively underrepresented — a pattern that mirrors, at the scale of the global literature, the specific characterization gaps identified for Paipa–Iza through the structured knowledge-gap diagnostic (Section 4.7).

The same synthesis was used to compile a structured global inventory of 326 named geothermal prospects. Of these, 229 systems had sufficient publicly reported information across all four GMI dimensions (project status, plant infrastructure, resource use, and breadth of technical characterization) to be scored using the scales in Tables 1–4, yielding an empirical benchmark distribution against which Paipa–Iza and the six comparative analogues are positioned in Section 3.9. For consistency with the narrative, evidence-based scoring applied to Paipa–Iza and the six analogues (Section 3), the fourth GMI dimension for the 229-system benchmark was proxied by the number of distinct technical-study categories documented for each system (geophysics, geochemistry, geology, well and log data, laboratory analysis, numerical modeling, engineering studies, advanced sensing, and hydrogeology), mapped onto the same five-class scale defined in Table 4.

2.2 Comparative workflow and phase description

The core methodological process was structured into four sequential phases, transitioning from macro-scale data compilation to the extraction of localized, transferable insights. This workflow is illustrated in Fig. 2.

Phase 1: Identification and Selection of Analogues: This phase begins with the screening and selection of specific geothermal analogues from the main dataset based on strict criteria of geological similarity and high data availability. This initial step ensures that only systems with structural and thermal conditions truly comparable to Paipa–Iza are integrated into the deep comparative analysis.

Phase 2: Technical Characterization: A rigorous technical characterization of each selected system is performed using standardized variables, including specific reservoir conditions and thermal properties. This step establishes a coherent, unified dataset that enables direct, unbiased comparison between fields.

Phase 3: Multidimensional Comparison: A transverse analysis is executed to identify key patterns, similarities, and critical deviations among the geothermal systems. This stage relies on a comparative matrix to support the cross-cutting interpretation of reservoir behavior across differing geological contexts.

Phase 4: Identification of Transferable Insights: The final phase centers on extracting practical lessons, including engineering insights, precise applicability to the PIGS framework, and strategic recommendations for geothermal exploration.

The overall workflow culminates in the generation of a structured comparative matrix and a robust set of transferable technical guidelines, as summarized in the final stage of the methodology (Fig. 2).

2.3 Geothermal Maturity Index (GMI)

Existing geothermal classification schemes—primarily based on reservoir enthalpy or temperature—conflate systems at vastly different stages of exploration and development, thereby constrain meaningful comparison between, for example, a field with four decades of production data and one still at the surface-reconnaissance phase. To address this gap, we introduce the Geothermal Maturity Index (GMI): a composite indicator designed to benchmark geothermal systems across four complementary dimensions that collectively capture the degree of technical and operational development, independent of reservoir temperature.

The GMI construction follows technical guidance on geothermal development stages and composite indicator methodology. OLADE technical guidance distinguishes reconnaissance, prefeasibility, feasibility, development, commissioning, and operation as progressive stages characterized by increasing geological knowledge, direct subsurface evidence, infrastructure, and resource use (Cozzini, 1994) OECD guidance for composite indicator development establishes the need for conceptually grounded dimensions, explicit and reproducible scoring criteria, normalization to a common scale, transparent aggregation, and sensitivity analysis [3]. Each of these steps is documented below.

2.3.1 Variables and Scoring Criteria

The GMI is constructed from four variables representing key dimensions of geothermal development: project development status, geothermal plant or infrastructure, final resource use, and level of technical characterization. Each variable was discretized into categorical classes reflecting increasing levels of maturity and assigned a normalized score between 0 and 1. The scoring scheme was designed to ensure internal consistency across variables, avoiding abrupt or arbitrary transitions, and reflecting a gradual progression in system maturity. The scoring criteria for each variable are described below and summarized in Tables 1–4 (Categories are ordered from lowest to highest maturity to ensure interpretability and internal consistency of the index.)

The first variable, *project development status*, captures the lifecycle stage of the geothermal project, from initial identification of surface manifestations through to full commercial operation. The scoring reflects the progressive reduction of resource uncertainty and the increasing commitment of technical and financial capital. The non-monotonic assignment of 0.5 to "Suspended" (above "Advanced Exploration" at 0.40) reflects the premise that a temporarily

suspended project retains institutional knowledge, existing infrastructure, and subsurface data—assets that distinguish it from one still in pre-feasibility. Abandoned projects (0.20) score below initial exploration because the irreversible loss of wells, data, and institutional capacity effectively resets the system closer to a reconnaissance baseline. The corresponding scoring scheme is presented in Table 1.

Table 1
Scoring scheme for project development status.

Category	Score
Preliminary recognition / surface manifestations	0.1
Abandoned / closed	0.2
Initial exploration (geophysical survey, first wells)	0.3
Advanced exploration / prefeasibility studies	0.4
Suspended project (temporary halt)	0.5
Resource confirmation (production tests)	0.6
Development / construction phase	0.8
Commercial operation	1

The second variable considers the *type of geothermal plant or infrastructure implemented*, which reflects the technological complexity of implemented energy conversion infrastructure, serving as a proxy for the degree of engineering commitment and market integration achieved by the system. Higher scores are associated with more sophisticated conversion technologies that enable electricity generation; lower scores correspond to the absence of infrastructure or to simple direct-use installations. The progression from 0 (no infrastructure) to 1 (hybrid plant) parallels the standard typology of geothermal plant technologies recognized by IRENA (2017) (Table 2).

Table 2
Scoring scheme for infrastructure implementation.

Category	Score
No infrastructure	0.0
Direct-use systems	0.2
Geothermal Pilot Plant	0.3
Dry Steam	0.4
Single Flash	0.6
Double Flash	0.7
Binary / ORC	0.9
Hybrid	1

The third variable evaluates the *final resource use* of the geothermal system, capturing the degree of functional integration into productive or energy systems. This dimension recognizes that a system exploited solely for balneological purposes represents a lower level of energy cascading and economic valorization than one supplying district heating or generating electricity. The scoring ladder is consistent with the utilization categories used in national and international geothermal statistics. The associated scoring scheme is detailed in Table 3.

Table 3
Scoring scheme for Final resource use.

Category	Score
No current use	0
Balneology / tourism	0.4
Agriculture	0.5
Heating / direct use	0.7
Mixed use	0.9
Electricity generation	1

The fourth variable assesses the *level of technical characterization* quantifying the breadth of analytical methods applied to characterize the geothermal system, including geological mapping, structural analysis, geochemical sampling and modelling, geophysical surveys (MT, gravity, magnetics, seismic), petrophysical measurements, and numerical reservoir modelling. A broader toolkit indicates a higher degreaee of epistemic maturity—that is, a system

whose behavior is constrained by multiple independent lines of evidence. The five-class ordinal scale (0 to ≥ 8 tools) was defined to align with the characterization phases recognized in international geothermal assessment guidelines. The scoring criteria are presented in Table 4.

Table 4
Scoring scheme for Level of Technical Characterization.

Category	Score
Up to 1 tool applied	0
2–3 tools applied	0.25
4–5 tools applied	0.5
6–7 tools applied	0.75
More than 8 tools	1

2.3.2 Uncertainty and sensitivity analysis.

The robustness of the Geothermal Maturity Index was assessed through a combination of deterministic weighting scenarios and Monte Carlo simulation. The analysis addressed three principal sources of methodological uncertainty: (i) the relative weighting assigned to the four GMI dimensions; (ii) uncertainty in the categorical score assigned to each system; and (iii) alternative procedures for consolidating the Paipa and Iza sectors into a single system-level score.

Six deterministic weighting scenarios were evaluated. The baseline scenario assigned equal weights of 0.25 to project status, infrastructure, final resource use, and technical characterization. Alternative scenarios emphasized exploration and knowledge acquisition, project implementation, development status, resource utilization, or technical characterization. All weighting vectors were constrained to sum to unity.

A Monte Carlo simulation comprising 50,000 realizations was subsequently performed. In each realization, the four component weights were sampled from a symmetric distribution which preserved a mean weight of 0.25 for each component while allowing variation around the equal-weight configuration. This distribution also ensured that all weights remained non-negative and summed to one.

Because the GMI component scores represent ordinal categories rather than continuous physical measurements, score uncertainty was modeled using discrete distributions. Each nominal score was allowed to remain unchanged or shift to the immediately adjacent lower or upper category. The transition probabilities were determined by the confidence assigned to the supporting evidence. High-confidence assignments were given probabilities of 0.05, 0.90, and 0.05 for the lower, nominal, and upper categories, respectively; medium-confidence assignments used probabilities of 0.15, 0.70, and 0.15; and low-confidence assignments used probabilities of 0.25, 0.50, and 0.25. At the limits of the scoring scale, probability mass corresponding to values outside the permissible range was retained at the boundary category.

For each realization, the GMI was calculated as:

$$GMI_i^{(k)} = \sum_{j=1}^{4} w_j^{(k)} s_j^{(k)}$$

Where $w_j^{(k)}$ is the simulated weight of component, $s_j^{(k)}$ is the simulated component score for geothermal system i, and k denotes the Monte Carlo realization. The simulation outputs included the median GMI, standard deviation, 2.5th and 97.5th percentiles, maturity-class probabilities, mean rank, and the probability of retaining the deterministic rank and maturity class. Ranking robustness was evaluated by calculating the Spearman correlation between the deterministic ranking and the ranking obtained in each realization. Input influence on the Paipa–Iza GMI was assessed using Spearman rank correlations between the simulated inputs and the resulting index.

Additional deterministic tests evaluated three alternative maturity-class threshold configurations and four approaches for integrating Paipa and Iza: using Paipa as the representative sector, calculating the component-wise average of Paipa and Iza, adopting the minimum component values as a conservative case, and applying an evidence-weighted average.

2.3.3 Index Calculation

The Geothermal Maturity Index (GMI) was calculated using an additive aggregation method expressed as the arithmetic mean of the four variables:

$$\varvec{GMI} = \frac{\varvec{S_{status}} + \varvec{S_{physical}} + \varvec{S_{use}} + \varvec{S_{technical}}}{4}$$

This formulation is consistent with established practices in synthetic indicator construction (OECD, 2008) allowing the integration of multiple dimensions into a single comparable metric. As a result, five maturity categories were defined based on the GMI result as shown below:

Table 5
Maturity categories based on GMI result.

Category	Interval	Maturity level
A	GMI ≥ 0.8	Very high maturity
B	0.60 ≤ GMI < 0.80	High maturity
C	0.40 ≤ GMI < 0.60	Intermediate maturity
D	0.20 ≤ GMI < 0.40	Low maturity
E	GMI < 0.20	Very low maturity

The GMI enables the positioning of geothermal systems along a continuous maturity trajectory, independent of reservoir temperature alone, thereby facilitating comparison across systems with different thermal regimes and geological contexts. In addition, geothermal plant typologies and resource utilization categories were aligned with internationally recognized classifications (Ito and Ruiz, 2017), ensuring consistency with global geothermal assessment frameworks.

2.4 Analytical Procedure

The comparative analysis was carried out through a structured and sequential methodological approach, designed to move from the detailed characterization of individual systems to the identification of transferable insights applicable to the Paipa–Iza geothermal system.

Initially, each geothermal analogue was characterized using a standardized set of variables that captured its fundamental technical and geological attributes. This characterization included the identification of the heat source and hydrothermal regime, the tectonic and geological context, reservoir temperature and depth, development stage and applied technologies. The information was systematically compiled and organized into a structured comparative matrix, ensuring consistency across all analyzed systems.

Building on this standardized dataset, a multidimensional comparative analysis was then performed to identify patterns, similarities, and critical differences between systems. Rather than re-describing individual attributes, this stage emphasized the interpretation of relationships across key dimensions, including geological–tectonic structure, thermal regime, technological development, energy utilization, and management strategies. This approach enabled the identification of coherent development patterns and system behaviors relevant to geothermal resource assessment.

2.5 Data Processing Tools

Data organization, normalization, and indicator calculations were performed using Microsoft Excel and Microsoft Power BI. These tools enabled structured database management, parameter filtering, similarity analysis, and visualization of comparative indicators, including the GMI.

Geographic Information Systems and geothermal reservoir modeling software were referenced exclusively in reviewed case studies and were not directly applied within this study.

3. Results

Given that no single geothermal field reproduces the complete hybrid configuration inferred for Paipa–Iza, analogue selection was conducted using a modular rather than a whole-system similarity approach. Each selected field represents one or more critical components of the Paipa–Iza conceptual model, including sedimentary reservoir architecture, fault-controlled permeability, non-volcanic hydrothermal circulation, magmatic heat supply, direct-use development, reinjection management, and mature electricity generation. Aachen was retained as an exploration-stage and fault-controlled circulation analogue; the German Molasse and North German basins as sedimentary-reservoir and connectivity analogues; the Pannonian Basin as a direct-use and reinjection analogue; Cerro Prieto as a structurally segmented reservoir-management analogue; and Central Tuscany as a magmatic–hydrothermal and mature operational end member. The analogue set was therefore designed to maximize complementary process coverage rather than to identify six fields with equal overall similarity to Paipa–Iza.

3.1 Paipa – Iza Geothermal System (PIGS)

The PIGS is characterized as a low-medium enthalpy system with temperatures in the range of 65 to 90°C. It is situated at an elevation of approximately 2525 m a.s.l. within a northward-tilted structural depression draining toward the Chicamocha River (Alfaro-Valero et al., 2019, pp. 161–165). The stratigraphy is primarily composed by Cretaceous sedimentary formations intruded by felsic magmas and, in some areas, overlain by pyroclastic deposits and dome complexes (Alfaro-Valero et al., 2019, pp. 170–176).

The PIGS is located along the axial zone of the Eastern Cordillera of Colombia, within a deformed Andean sedimentary basin shaped by Cenozoic compressional tectonics (Alfaro et al., 2020, p. 1). This basin features a thick Cretaceous–Cenozoic sedimentary rocks overlying a Paleozoic metamorphic basement associated with the Floresta Massif (Gilbert, 2019, p. 2).

This stratigraphic sedimentary record is composed of alternating sandstones, shales and limestones. The Une Formation (Lower Cretaceous) and Guadalupe Group (Upper Cretaceous) are particularly important, as they represent the most permeable units regionally and serve as the primary sedimentary reservoirs within the geothermal system (Beltrán, 2015, p. 27). The basin architecture is strongly influenced by a fault network comprising high-angle reverse and normal faults, including the Boyacá, Soapaga, Paipa-Iza, Cerro Plateado, Las Peñas, and Agua Tibia faults. This fault network segments both the basement

and sedimentary cover, controls permeability anisotropy, and establishes a structural framework for deep fluid circulation and vertical hydraulic connectivity (Gilbert, 2019, pp. 2–3).

From a thermal and magmatic perspective, the Paipa-Iza geothermal field represents a unique geological setting in Colombia. Unlike geothermal systems associated solely with active volcanic arcs, Paipa-Iza is characterized by the presence of Miocene-Pleistocene felsic intrusions within the Cretaceous-Tertiary sedimentary sequence of the Paipa-Iza Complex. These intrusions likely constitute a long-lived magmatic heat source (Alfaro et al., 2010, p. 1). Integrated magnetotelluric, gravimetric, and magnetic studies reveal resistivity and density anomalies consistent with both shallow and deep intrusive bodies, as well as zones of enhanced heat transfer. This supports the interpretation of a thermally anomalous crust beneath the geothermal area (Gilbert, 2019, pp. 7–8), (Beltrán, 2015, pp. 103–110).

Furthermore, geochemical and mineralogical analyses of drilling cores have documented significant enrichments in U, Th, and K within intensely altered intrusions, particularly in the El Durazno sector. This indicates a non-negligible radiogenic heat contribution that augments regional heat flow and distinguishes Paipa-Iza from purely sedimentary geothermal systems (Alfaro-Valero et al., 2019, p. 170).

3.1.1 Magmatic and volcanic components.

As previously mentioned, Paipa-Iza is not solely a sedimentary basin geothermal system; it is also influenced by felsic magmatism expressed as dome complexes and intrusions. Previous research by SGC suggests that the system involves a primary magmatic heat source, along with a potential radiogenic contribution from U-Th-K-enriched igneous rocks (El Durazno intrusion) (Alfaro-Valero et al., 2019, pp. 170–175). Preliminary models similarly propose a magmatic heat source dating back approximately 2.5–2.1 million years, linking magma ascent pathways to extensional basement faults (Paipa–Iza and Cerro Plateado) (Alfaro et al., 2010, pp. 1, 3).

Rueda-Gutierrez documents petrography dominated by K-feldspar (sanidine/anorthoclase) + plagioclase (albite) + amphibole (hornblende) + biotite, with variable kaolinite replacement (especially in feldspars). This is consistent with hydrothermal alteration overprints on felsic domes (Rueda-Gutiérrez, 2020, p. 51). The same author reports 40Ar/39Ar ages for Alto Los Volcanes and Quebrada Honda at approximately 1.76 and 1.8 million years, respectively, and for Alto Los Godos at approximately 2.8–2.6 million years. This indicates at least two Late Pliocene-Early Pleistocene magmatic pulses (Rueda-Gutiérrez, 2020, pp. 73–74). This time-transgressive dome emplacement is significant because it supports a multi-pulse thermal history rather than a single, short-lived heating event.

A complementary petrological study of the Paipa Volcanic Complex suggests that felsic magmas are best explained by the melting of local (meta)sedimentary basement under H_2O-saturated conditions at middle-crustal pressures (approximately 1.3 GPa) and 690–740°C (Errázuriz-Henao et al., 2024, pp. 1–3). While the scope of the PVC extends beyond the immediate geothermal manifestation, the inference of water-fluxed crustal melting is important. It implies a volatile-rich magmatic environment that can sustain hydrothermal circulation and contribute magmatic/thermogenic gases, which complicate surface geochemical signatures.

3.2 Cerro Prieto

The Cerro Prieto Geothermal Field (CPGF) is a mature, high-enthalpy (350–370°C), liquid-dominated system in the transtensional Salton Trough, with 720 MWe installed capacity and commercial production since 1973 (Lippmann et al., 1999; Helio and Cfe, 2000). The reservoir is hosted in deltaic sandstones sealed by low-permeability shales, and productivity is controlled by four major structural blocks segmented by the Fault H system, which define corridors of enhanced permeability within an otherwise sedimentary host rock (Aguilar, 2006; Glowacka et al., 2005). Reinjection, initiated in 1986, has mitigated pressure decline without significant productivity loss, supported by decades of reservoir-engineering refinement (Puente and Ribo-Muñoz, 1994; De León Vivar et al., 2001).

Implications for Paipa–Iza

Cerro Prieto demonstrates that structural block segmentation and fault-associated permeability corridors can govern fluid upflow and recharge in a mature industrial field, independent of the specific tectonic setting. At Paipa–Iza, the major fault network and basement–cover connectivity could play an analogous role in organizing deep circulation, offering a reference for how an integrated structure–reservoir–management approach supports long-term production and injection sustainability.

3.3 German Molasse Basin (GMB)

The German Molasse Basin (GMB) is Germany's most industrially developed geothermal province, a deep, medium-enthalpy (130–160°C) hydrothermal system formed as an Alpine foreland wedge basin (Agemar et al., 2018; Krumbholz et al., 2024). The primary reservoir is the Upper Jurassic (Malm) carbonate aquifer, where matrix permeability is very low (< 1.4 mD) and productivity depends almost entirely on secondary porosity created by fracturing, karstification, and fault segmentation associated with structures such as the Munich Fault (Wadas and von Hartmann, 2022; Bohnsack et al., 2021). Heat transfer combines regional conduction with fault- and karst-controlled convection, and reinjection is essential for pressure balance and thermal sustainability (Azzola and Gaucher, 2024; Schölderle et al., 2021).

Implications for Paipa–Iza

The GMB confirms that productivity in structurally controlled hydrothermal systems depends less on matrix permeability than on secondary fracture/karst networks and fault segmentation. Paipa–Iza shares this dependence on effective connectivity, and the GMB experience underscores that resolving this

heterogeneity requires integrated geophysical and structural characterization rather than porosity data alone.

3.4 North German Basin (NGB)

The North German Basin (NGB) is a deep, non-magmatic, low- to medium-enthalpy hydrothermal system (80–140°C) hosted in Mesozoic sandstones and deeper Permian (Rotliegend) reservoirs within an intracratonic sag basin shaped by Zechstein salt tectonics (Norden et al., 2023; Mantei et al., 2025). Heat originates from the regional geothermal gradient (~ 60–80 mW/m², locally enhanced above salt structures), with no active magmatic source; productivity relies on facies continuity and net sand thickness (up to 1 Darcy permeability in favorable channel belts) rather than fault-dominated flow, as demonstrated by 3D seismic surveys at Groß Schönebeck (Norden et al., 2023; Mantei et al., 2025). Development has progressed from repurposed hydrocarbon wells to multi-well doublet arrays, with EGS/petrothermal stimulation tested in low-permeability volcanic basement (Agemar et al., 2018).

Implications for Paipa–Iza: The NGB is a structurally important counterpoint: although Paipa–Iza's conceptual model emphasizes fault control, the NGB shows that heterogeneous sedimentary basins can instead be governed by depositional architecture and facies continuity. The Une Formation could plausibly exhibit comparable stratigraphic controls that have not yet been evaluated independently of the structural framework, and the NGB's instrumentation practices offer a template for reducing this uncertainty.

3.5 Aachen, Germany.

Aachen is a low-enthalpy (up to ~ 85°C at 2500 m), non-magmatic, convection-dominated system at the northern edge of the Variscan deformation front, where Devonian carbonates (Massenkalk) and underlying siliciclastic units exhibit extremely low matrix permeability (< 1%) (Dijkshoorn et al., 2013; Gomez-Diaz et al., 2025). Productive behavior is entirely fracture- and fault-dominated: thermal springs (up to ~ 72°C) emerge along NW–SE structures such as the Lousberg fault zone, and detachment-fault geometries are interpreted to control connectivity and compartmentalization (Jüstel et al., 2022; Gómez Díaz et al., 2024; Balcewicz et al., 2021).

Implications for Paipa–Iza

Aachen demonstrates that a convective, fault-controlled system can sustain significant surface manifestations without any magmatic heat source, confirming that structural permeability—not the presence of intrusions—is the necessary condition for circulation and surface expression. This is a critical interpretive counterpoint for Paipa–Iza, where the magmatic component must not be assumed sufficient on its own to explain fluid pathways.

3.6 Pannonian Basin – Hungary

The Pannonian Basin (Hungary) is a deep, non-magmatic, low- to medium-enthalpy system (100–200°C) shaped by lithospheric thinning and asthenospheric upwelling, producing heat flow up to twice the global average (Lenkey et al., 2021; Szanyi et al., 2026). Two reservoir types coexist: high-porosity Neogene porous sandstones (22–31% porosity, hundreds to thousands of mD) and fractured/karstified Mesozoic carbonate and crystalline basement, where transmissivity depends entirely on the fracture network (Njeru et al., 2024; Nur Ali Akbar et al., 2022). Development has evolved toward cascading direct-use schemes (district heating, agro-industry, balneology) rather than electricity generation, and decades of production with limited reinjection at fields such as Szentes produced measurable hydraulic head decline and reinjection-clogging risks that now require dedicated treatment infrastructure (Strasszer and Xydis, 2024; Bálint and Szanyi, 2015; Markó et al., 2021).

Implications for Paipa–Iza

The Pannonian Basin shows that low-to-medium enthalpy resources can generate substantial value through direct-use and cascading schemes without requiring electricity generation—directly relevant given Paipa–Iza's existing balneological and tourism profile. It also demonstrates that reinjection design and clogging risk should be treated as early engineering variables rather than deferred decisions.

3.7 Central Tuscany: Larderello–Travale and Monte Amiata, Italy

Larderello–Travale is a vapor-dominated, high-enthalpy system (150–260°C in the shallow reservoir, 300–350°C at depth, locally exceeding 400°C) hosted in a stack of Alpine nappes over metamorphic and intrusive basement, segmented by NW–SE normal faults and SW–NE transfer zones (Batini et al., 2003; Saccorotti et al., 2014; Liotta et al., 2025). Two hydraulically connected reservoirs occur: a shallow one in tectonic breccias and evaporites (500–1500 m), and a deep one in fractured metamorphic basement and granitic intrusions (2000–4500 m), with permeability governed almost entirely by fracturing and karstification (Bellani et al., 2004; Della Vedova et al., 2008). The heat source is a composite granitic batholith emplaced since the Pliocene, with the K-Horizon marking the brittle–ductile transition and partially molten intrusive roofs (Santilano et al., 2016; Boyce et al., 2003). Despite over a century of exploitation, mass production has remained remarkably stable (~ 3000 t/h since 1951), attributed to long-circuit meteoric recharge and limited condensate reinjection since 1979 (Liotta et al., 2025; Minissale, 1991).

Monte Amiata is likewise high-enthalpy (150–230°C shallow, 300–360°C deep) but water-dominated, with localized CO_2-rich gas traps, hosted in a dual-reservoir configuration (shallow carbonate–evaporite, deep metamorphic) separated by a partial hydraulic barrier (Fulignati et al., 2014; Belgiorno et al., 2019). Surface heat flow reaches up to ~ 600 mW/m², and industrial exploitation since 1959 (121 MWe installed) relies on flash plants with partial reinjection (one quarter to one half of produced fluids). A documented decline of 200–300 m in the volcanic freshwater aquifer, driven by depressurization propagating through vertically connected faults, illustrates strong coupling between the deep reservoir and shallow water resources (Borgia et al., 2022; Mazzoldi et al., 2015).

Implications for Paipa–Iza: The Tuscan analogues demonstrate that a composite intrusive heat source can sustain very high enthalpies and complex dual-reservoir systems, informative for understanding how Paipa–Iza's felsic intrusions could behave over geological time—though the much lower observed temperatures (65–90°C) indicate a far earlier stage of thermal maturity. They also introduce an environmental dimension largely absent from the other analogues: Monte Amiata's documented aquifer decline and the need for dedicated gas-emissions management (H_2S, Hg) show that systems with an igneous heat source and volatile-rich melting require environmental and hydrogeological baseline assessment from the earliest exploration stages—directly relevant given the volatile-rich crustal melting inferred for the Paipa Volcanic Complex.

3.8 Comparative Synthesis of GMI Scores Across Analogues

Table 6 consolidates the four GMI component scores and the resulting composite index for Paipa–Iza and the six international analogue cases, providing a quantitative overview of the comparative data presented in Sections 3.1 to 3.7. The highest GMI values are observed in Central Tuscany (1.0), Cerro Prieto (0.975), The Pannonian Basin (0.8875), reflecting their commercial operational status, well-established electrical infrastructure, and advanced levels of technical investigation. German basins GMB/NGB (0.6625) and Aachen (0.525) exhibit a intermediate degree of maturity, although their development is primarily oriented toward direct-use applications and heating systems. In contrast, Paipa–Iza (0.3625) remains at early-stage or prefeasibility phases, characterized by some technical characterization but lacking consolidated infrastructure and industrial - scale use.

Table 6
Comparison (PIGS vs. analogues) under the parameters of the GMI

System	(1) Current project status (Score)	(2) Type of geothermal plant or infrastructure (Score)	(3) Final resource use (Score)	(4) Level of advanced technical studies (Score)	(5) GMI (0–1)	(6) Summary analysis
Paipa–Iza (PIGS)	Initial exploration (0.3). System under characterization and at an early stage; no commercial operation or installed capacity is reported (Alfaro et al., 2010; Alfaro et al., 2020).	No infrastructure (0.0). No electric or thermal plants are reported as installed; the geological architecture and structural/hydrothermal framework are described (Alfaro et al., 2010; Alfaro et al., 2020).	Balneology / tourism (0.4). The system is framed around thermal manifestations and spa-oriented direct uses (Alfaro et al., 2010; Alfaro et al., 2020).	6–7 tools (0.75). Integrates magnetotellurics, gravimetry, magnetometry, geochemistry, drill-core mineralogy, and structural characterization (Alfaro et al., 2010; Alfaro et al., 2020).	0.3625	Early-stage maturity is constrained by the absence of infrastructure and the still-developing project status; integrated characterization already supports discussion of heat-source partitioning and hydraulic connectivity.
Cerro Prieto	Commercial operation (1.0). Mature field in commercial production; the table indicates production since 1973, expansion up to 720 MWe, and reinjection since 1986 (Lippmann et al., 1999; Puente and De La Pena, n.d.).	Binary / ORC (0.9). Electric-power infrastructure associated with a large-scale industrial field; reinjection is also emphasized (Lippmann et al., 1999; Puente and De La Pena, n.d.).	Electricity generation (1.0). The dominant end use is electricity; the table does not emphasize direct thermal use as the main purpose (Lippmann et al., 1999; Puente and De La Pena, n.d.).	≥ 8 tools (1). Integrated geophysical campaigns, 3D structural updates supported by extensive drilling, and 3D thermo-hydraulic numerical modeling (Lippmann et al., 1999; Puente and De La Pena, n.d.).	0.975	A high-maturity case shaped by long-term operation, reinjection, and integrated geophysical/structural modeling; it is a useful benchmark for sustainable pressure support.
German Molasse Basin (GMB)	Commercial operation (1.0). The region is described as Germany's most developed geothermal area (Agemar et al., 2018), (Schölderle et al., 2021) .	Direct-use systems (0.2). Doublet/multi-well schemes, deviated wells, ESP pumps, and fiber-optic monitoring dominate; binary electricity is presented as moderately feasible (Agemar et al., 2018; Schölderle et al., 2021)	Heating / direct use (0.7). District heating is the dominant end use; electrical use is moderate and mainly via binary cycles (Agemar et al., 2018; Schölderle et al., 2021).	6–7 tools (0.75). Highlights include 3D seismic, amplitude inversion for 3D porosity models, and distributed DTS/DAS monitoring (Agemar et al., 2018; Schölderle et al., 2021).	0.6625	Shows that maturity can also be achieved under direct-use paradigms when 3D imaging and monitoring reduce reservoir uncertainty.
North German Basin (NGB)	Commercial operation (1.0). There are multiple operational projects and EGS tests in specific contexts (Mantei et al., 2025; Shatyrbayeva et al., 2024).	Direct-use systems (0.2). Typical infrastructure includes doublets and multi-well arrays, with ESP use, heat pumps, and limited ORC/binary electricity generation (Mantei et al., 2025; Shatyrbayeva et al., 2024).	Heating / direct use (0.7). Direct thermal use predominates; electricity generation is secondary and limited (Mantei et al., 2025; Shatyrbayeva et al., 2024).	6–7 tools (0.75). Includes a 2D→3D seismic transition, 3D models, subsalt imaging, and DAS/DTS monitoring (Mantei et al., 2025; Shatyrbayeva et al., 2024).	0.6625	Emphasizes that multi-well design, monitoring, and facies/thickness controls can be as critical as major faults for performance and sustainability.
Aachen (Germany)	Advanced exploration / prefeasibility (0.4). Non-magmatic case under evaluation/exploration; industrial operation is not described (Gomez-Diaz et al., 2025).	No infrastructure (0). The main infrastructure mentioned is the RWTH1 deep well; no power plant is reported (Gomez-Diaz et al., 2025).	Heating / direct use (0.7). Thermal manifestations indicate circulation, but no industrial utilization scheme is detailed (Gomez-Diaz et al., 2025).	≥ 8 tools (1.0). Seismic reprocessing, a structural conceptual model, thermal logs, hydrogeochemistry, fluid inclusions, and petrophysical properties are reported (Gomez-Diaz et al., 2025).	0.525	A useful analogue showing that strong characterization can coexist with limited utilization and infrastructure at the exploration stage.
Pannonian Basin (Hungary)	Commercial operation (1.0). Development has a strong direct-use component and incipient electricity generation; one operating plant in Tura is mentioned, (Bálint and Szanyi, 2015; Markó et al., 2021; Strasszer and Xydis, 2024; Békési et al., 2022).	Binary / ORC (0.9). Includes wells in porous aquifers, submersible pumps, district-heating schemes, and ORC for medium-enthalpy resources; EGS potential is also discussed (Bálint and Szanyi, 2015; Markó et al., 2021; Strasszer and Xydis, 2024; Békési et al., 2022).	Mixed use (0.9). Cascading uses combine heating, agriculture/industry, and balneology, with thermal use predominating (Bálint and Szanyi, 2015; Markó et al., 2021; Strasszer and Xydis, 2024; Békési et al., 2022).	6–7 tools (0.75). Reported studies include potential assessment methods, modeling, reinjection analysis, and EGS workflows (Bálint and Szanyi, 2015; Markó et al., 2021; Strasszer and Xydis, 2024; Békési et al., 2022).	0.8875	Supports the sustainability discussion by highlighting reinjection risks, clogging/scaling issues, and the need for monitoring/diagnostics.
Central Tuscany (Larderello–Travale &	Commercial operation (1.0). Mature fields with industrial history; later electricity	Hybrid (1.0). Power plants, AMIS environmental management, and	Electricity generation (1.0). Electricity is the dominant end use, with residual-heat	≥ 8 tools (1.0). The table reports deep horizons, geophysical	1.0	Represents the high-enthalpy operational end member, where infrastructure

System	(1) Current project status (Score)	(2) Type of geothermal plant or infrastructure (Score)	(3) Final resource use (Score)	(4) Level of advanced technical studies (Score)	(5) GMI (0–1)	(6) Summary analysis
Monte Amiata, Italy)	production in Larderello–Travale and industrial exploitation since 1959 in Monte Amiata are reported (Saccorotti et al., 2014; Taussi et al., 2023; Della Vedova et al., 2008; Fulignati et al., 2014; Magi et al., 2019; Borgia et al., 2022).	partial/marginal reinjection with a total-reinjection goal are reported (Saccorotti et al., 2014; Taussi et al., 2023; Della Vedova et al., 2008; Fulignati et al., 2014; Magi et al., 2019; Borgia et al., 2022).	uses such as district heating/greenhouses also mentioned (Saccorotti et al., 2014; Taussi et al., 2023; Della Vedova et al., 2008; Fulignati et al., 2014; Magi et al., 2019; Minissale, 1991; Somma et al., 2017; Borgia et al., 2022).	evidence including EM/MT, complex tectono-stratigraphic models, and hydro-environmental management (Saccorotti et al., 2014; Taussi et al., 2023; Della Vedova et al., 2008; Fulignati et al., 2014; Magi et al., 2019; Minissale, 1991; Somma et al., 2017; Borgia et al., 2022).		complexity and environmental management become central to maturity.

Key comparative findings

The highest GMI values are observed in Central Tuscany (1.0), Cerro Prieto (0.975), The Pannonian Basin (0.8875), reflecting their commercial operational status, well-established electrical infrastructure, and advanced levels of technical investigation. German basins GMB/NGB (0.6625) and Aachen (0.525) exhibit a intermediate degree of maturity, although their development is primarily oriented toward direct-use applications and heating systems. In contrast, Paipa–Iza (0.3625) remains at early-stage or prefeasibility phases, characterized by some technical characterization but lacking consolidated infrastructure and industrial - scale use.

3.9 Sensitivity and Robustness of the GMI

The deterministic weighting analysis showed that the relative ordering of the geothermal systems was largely preserved under alternative conceptual definitions of maturity. For Paipa–Iza, the estimated GMI ranged from 0.308 under the implementation-oriented scenario to 0.500 when technical characterization received the dominant weight. The baseline equal-weight configuration produced a GMI of 0.3625. Scenarios emphasizing exploration and knowledge acquisition or technical characterization increased the Paipa–Iza score to 0.450 and 0.500, respectively, whereas scenarios emphasizing infrastructure and implementation reduced the index.

The Monte Carlo analysis confirmed that the comparative ranking was substantially more stable than the absolute maturity classification. Across 50,000 realizations, the mean Spearman correlation between the deterministic and simulated rankings was 0.972, with a 2.5th–97.5th percentile range of 0.912–1.000. Central Tuscany and Cerro Prieto remained predominantly within the highest-ranking positions, followed by the Pannonian Basin and the German sedimentary-basin systems. Paipa–Iza and Aachen remained concentrated in the two lowest positions.

Paipa–Iza presented a simulated median GMI of 0.353 and a 95% uncertainty interval of 0.198–0.487. The system remained within the low-maturity class in 73.9% of the realizations, shifted to the medium-maturity class in 23.4%, and fell within the very-low-maturity class in 2.7%. The probability of obtaining a GMI equal to or greater than the 0.40 medium-maturity threshold was 23.5%. Assignment to the high-maturity class was negligible.

The probability that Paipa–Iza obtained a higher GMI than Aachen was 73.0%, confirming its generally more advanced position among the two pre-infrastructure systems, although overlapping uncertainty intervals indicate that this distinction is not absolute. Paipa–Iza retained its deterministic sixth-ranking position in 74.9% of the simulations.

Sensitivity coefficients indicated that the Paipa–Iza result was most strongly influenced by the weight assigned to technical characterization ($\rho = 0.488$), the technical-characterization score itself ($\rho = 0.471$), and the final-use score ($\rho = 0.448$). Conversely, increasing the infrastructure weight reduced the index ($\rho = -0.438$), because no consolidated geothermal infrastructure is currently assigned to the system. The weight assigned to project status exerted comparatively little influence.

Alternative procedures for integrating Paipa and Iza produced GMI values between 0.250 and 0.363. The component-wise average resulted in a GMI of 0.306, the conservative scenario yielded 0.250, and the evidence-weighted scenario produced 0.329. All four integration approaches retained Paipa–Iza within the low-maturity class under the baseline classification thresholds.

3.9 Global Positioning of Paipa–Iza within the 229-System Benchmark

Applying the same four-dimension scoring scheme (Tables 1–4) to the extended benchmark dataset (Section 2.1.1) yields GMI values ranging from 0.075 to 0.975 across the 229 scored systems (mean = 0.502, median = 0.513, SD = 0.240), with systems distributed across the five maturity categories as follows: Very high, 13.5%; High, 23.6%; Intermediate, 27.5%; Low, 20.5%; Very low, 14.8%.

Within this distribution, the database-consistent scores obtained for Paipa (GMI = 0.300) and Iza (GMI = 0.250) both fall in the Low-maturity category, at the 25.3rd and 19.7th percentiles respectively; their component-wise average (GMI = 0.275) corresponds to the 22.3rd percentile. This independently, mechanically scored estimate is consistent with the narrative, evidence-weighted GMI of 0.3625 obtained for Paipa–Iza as a single representative unit

(Section 3.8), which occupies the 34.1st percentile of the same 229-system distribution, and with its Monte Carlo 95% uncertainty interval (0.198–0.487), spanning approximately the 15th to 46th percentiles. The convergence of these two independently derived estimates — one based on detailed narrative scoring of the primary literature specific to Paipa–Iza, the other on a mechanical count of documented technical studies across a 326-system global inventory — reinforces the low-maturity classification of Paipa–Iza and indicates that this result is not an artifact of subjective scoring.

The six comparative analogues occupy markedly higher positions within the same benchmark: Central Tuscany (GMI = 0.900, 96.9th percentile) and the North German Basin (GMI = 0.838, 92.1st percentile) rank among the most mature systems in the global inventory, followed by Cerro Prieto (0.800, 90.0th percentile), Aachen (0.725, 77.3rd percentile), the German Molasse Basin (0.650, 68.6th percentile), and the Pannonian Basin (0.600, 65.9th percentile). All six analogues therefore rank above the 65th percentile of the global maturity distribution, confirming that they were deliberately selected from the upper half of that distribution to illustrate development trajectories and transferable engineering lessons (Section 4), rather than to identify systems of comparable overall maturity to Paipa–Iza. This explicit positioning — a nascent, low-maturity hybrid system benchmarked against high-maturity analogues drawn from a 229-system global inventory — is, to the authors' knowledge, the first application of a composite, database-calibrated maturity index to a Colombian or broader Northern Andean geothermal prospect.

4. Discussion

4.1 Comparative framework and maturity-based interpretation

The results support the article's central hypothesis: the Paipa–Iza Geothermal System (PIGS) shares fundamental structural controls and hydrothermal architectures with geothermal fields exhibiting diverse enthalpy levels and operating within different tectonic settings. This similarity allows for the transfer of exploration, characterization, and operational management practices. This approach aligns with systematic review and comparative case-analysis methodologies, which are used to integrate heterogeneous evidence and extract replicable patterns (Snyder, 2019), (Yin and Campbell, 2018). Furthermore, the selection of variables (heat source, reservoir-seal lithology, manifestations, development stage, etc.) is consistent with evaluation frameworks employed by industry and international organizations (Ito and Ruiz, 2017), while the construction of a composite indicator (GMI) draws upon established guidelines for synthetic indices (OECD, 2008).

A key interpretive advantage of the proposed GMI is that it makes "maturity" explicit and comparable by translating four complementary dimensions—project status, infrastructure, end use, and technical characterization—into ordered categories with normalized scores. The scoring criteria are structured to avoid abrupt transitions and maintain internal consistency, enabling maturity to be interpreted as a gradual, multidimensional trajectory rather than a single-threshold attribute (Tables 1–4). The additive aggregation (arithmetic mean of the four components) supports transparent cross-case positioning and reinforces the broader premise that geothermal viability and readiness cannot be inferred solely from temperature (OECD, 2008). Plant typologies and utilization categories are also aligned with internationally recognized geothermal classifications, further strengthening consistency across analogue comparisons(Ito and Ruiz, 2017).

Rather than restating each analogue individually, the discussion that follows synthesizes the comparative evidence across three transversal axes that determine geothermal system behavior independently of enthalpy class: (i) the architecture and origin of the heat source, (ii) the structural and stratigraphic control of effective permeability, and (iii) the trajectory from characterization to sustainable exploitation. Paipa–Iza is positioned within each axis, and the GMI is used throughout as the quantitative backbone that anchors this synthesis (Table 6).

4.2 Comparison of the heat source architecture

The six analogues collectively span the full spectrum of heat-source configurations against which Paipa–Iza can be positioned. At one end, Central Tuscany (Larderello–Travale and Monte Amiata) represents the magmatic end member: a composite granitic batholith emplaced at shallow depth sustains a vapor- and liquid-dominated system with deep architectural markers (the K-Horizon) linked to the brittle–ductile transition and partially molten intrusive roofs (Saccorotti et al., 2014), (Taussi et al., 2023), (De Franco et al., 2019). At the opposite end, the North German Basin (NGB) and the Pannonian Basin represent non-magmatic, purely conductive-to-convective systems, where heat originates from the regional geothermal gradient, sediment thickness, and—in the Pannonian case—lithospheric thinning and asthenospheric upwelling, with no active intrusive body involved (Lenkey et al., 2021), (Szanyi et al., 2026), (Szijártó et al., 2021).

Paipa–Iza occupies an intermediate and conceptually distinct position within this spectrum. The compiled evidence indicates a hybrid heat source: Miocene–Pleistocene felsic intrusions and domes of the Paipa Volcanic Complex provide a long-lived magmatic component, while U–Th–K enrichment in altered intrusives points to a non-negligible radiogenic contribution superimposed on that magmatic budget (Alfaro et al., 2010), (Alfaro et al., 2020), (Gomez Romero, 2019), (González-Idárraga, 2021). This configuration does not map cleanly onto either end member. The Tuscan analogues demonstrate that a composite intrusive heat source can sustain very high enthalpies and complex dual-reservoir systems (Batini et al., 2003), (Saccorotti et al., 2014), (Bellani et al., 2004), (Taussi et al., 2023), (Minissale, 1991), which is informative for understanding how Paipa–Iza's intrusions could behave over geological time, but the much lower observed temperatures at Paipa–Iza (65–90°C) indicate that the system has not developed the same degree of thermal maturity, connectivity, or insulation as Tuscany. Conversely, the non-magmatic analogues (NGB, Pannonian Basin) confirm that conduction and regional heat flow alone can sustain low-to-medium enthalpy systems of considerable industrial relevance (Dijkshoorn et al., 2013), (Alfaro-Valero et al., 2019), (Gilbert, 2019), (Norden et al., 2023). without requiring an intrusive component—underscoring that the magmatic and radiogenic contributions at Paipa–Iza, however real, are not yet quantified relative to the baseline conductive regime expected for the Eastern Cordillera.

This comparative positioning exposes the most consequential open question for PIGS: the partitioning of heat between magmatic and radiogenic sources remains unresolved, and no analogue alone can settle it, because each end member isolates one mechanism that at Paipa–Iza appears to operate jointly

(Alfaro et al., 2010), (Alfaro-Valero et al., 2019), (Alfaro et al., 2020). Addressing this will require integrating petrophysics, geochemistry, and geophysics in a way that goes beyond what any single analogue comparison can offer (Gomez Romero, 2019).

4.3. Structural and stratigraphic control of effective permeability

Across all six analogues, a consistent pattern emerges: productivity is governed less by average reservoir porosity than by the spatial distribution of effective permeability, whether that permeability is structurally, stratigraphically, or diagenetically controlled. Three distinct sub-patterns are evident in the comparative record.

First, fault-dominated connectivity is illustrated by Cerro Prieto, where transtensional deformation and structural block segmentation define corridors of enhanced permeability within an otherwise sedimentary, sandstone-hosted reservoir sealed by clay-rich cap rock (Lippmann et al., 1999), (Glowacka et al., 2005). A directly comparable mechanism is proposed for Paipa–Iza, where the Guadalupe Group and the Une Formation constitutes the regionally permeable sedimentary unit and the hierarchical fault network (Boyacá, Soapaga, Paipa–Iza, Cerro Plateado) is interpreted as the primary control on vertical and lateral connectivity (Alfaro et al., 2010), (Gilbert, 2019), (Beltrán, 2015), (Alfaro et al., 2020). The Aachen analogue reinforces this same logic in a non-magmatic, carbonate-hosted setting: extremely low matrix permeability (< 1%) forces all productive behavior into fracture- and fault-damage zones, with thermal springs emerging precisely along major structural trends (Dijkshoorn et al., 2013), (Jüstel et al., 2022), (Gómez Díaz et al., 2024). That a convective, fault-controlled system can produce significant surface manifestations without any magmatic heat source is a critical interpretive counterpoint for Paipa–Iza: it demonstrates that structural permeability, not the presence of intrusions, is the necessary condition for sustained circulation and surface expression (Alfaro et al., 2010), (Alfaro et al., 2020), (Lippmann et al., 1999), (Minissale, 1991)

Second, discontinuity- and karst-dominated connectivity is exemplified by the German Molasse Basin (GMB), where Jurassic (Malm) carbonate reservoirs exhibit porosity reaching up to 20% but matrix permeability below 1.4 mD, such that productivity depends almost entirely on fracturing, karstification, and fault segmentation (Wadas and von Hartmann, 2022), (Krumbholz et al., 2024), (Bohnsack et al., 2021), (Freitag et al., 2022). This pattern is directly relevant to Paipa–Iza, where the hydrothermal overprint associated with the felsic intrusions suggests that part of the system—particularly near major structures and altered zones—may behave as a discontinuity-dominated medium analogous to the GMB, rather than as a simple porous sedimentary aquifer (Alfaro et al., 2010), (Alfaro et al., 2020), (Wadas and von Hartmann, 2022). The operational lesson from the GMB is unambiguous: resolving this kind of heterogeneity requires 3D seismic imaging, amplitude inversion, and integrated structural models, since productivity cannot be predicted from porosity logs alone (Wadas and von Hartmann, 2022), (Bohnsack et al., 2021).

Third, facies- and thickness-controlled connectivity is the dominant mechanism at the NGB, where 3D seismic surveys at Groß Schönebeck reveal an absence of large-displacement faults within the Rotliegend reservoir, shifting the primary control toward depositional architecture, net sand thickness, and lateral facies continuity (Norden et al., 2023), (Mantei et al., 2025), (Shatyrbayeva et al., 2024). This is a structurally important counterpoint for Paipa–Iza: although the fault network is emphasized throughout the available literature (Alfaro-Valero et al., 2019), (Gilbert, 2019), (Beltrán, 2015), (Errázuriz-Henao et al., 2024), the Une Formation could plausibly exhibit comparable stratigraphic-facies controls on connectivity that have not yet been evaluated with a sedimentological or geostatistical approach, independent of the structural framework .

Taken together, these three patterns indicate that Paipa–Iza cannot be assumed a priori to behave as a purely fault-controlled system simply because its conceptual model emphasizes major faults. The GMB and NGB analogues both demonstrate that heterogeneous sedimentary basins frequently combine structural, diagenetic, and depositional controls in ways that are only resolved through integrated 3D characterization—precisely the kind of multidimensional technical maturity that the GMI's fourth variable (level of technical characterization) is designed to capture (Alfaro et al., 2010), (Gilbert, 2019), (Beltrán, 2015), (Wadas and von Hartmann, 2022), (Norden et al., 2023).

4.4 Characterization and Sustainable Production

The comparative dataset also traces a development trajectory that is directly informative for Paipa–Iza's current pre-commercial stage. Mature, high-GMI systems converge on a small set of operational priorities once initial exploitation begins, and the timing of their adoption—early versus reactive—differentiates successful long-term management from costly retrofitting.

Reinjection emerges as the single most consistent lesson across the dataset. At Cerro Prieto, reinjection initiated in 1986 has mitigated pressure decline without significant productivity loss in a field that has sustained commercial operation since 1973 (Rosales, 2001), (Helio and Cfe, 2000). In the Pannonian Basin, by contrast, decades of production with limited reinjection at fields such as Szentes produced measurable hydraulic head decline and documented surface deformation, while reinjection itself introduced a distinct risk: clogging through physical, chemical, and biological mechanisms that demands dedicated treatment and monitoring infrastructure (Njeru et al., 2024), (Bálint and Szanyi, 2015), (Markó et al., 2021), (Szolga et al., 2024). Central Tuscany illustrates an intermediate case: marginal and condensate reinjection at Larderello–Travale, and partial reinjection (one quarter to one half of produced fluids) at Monte Amiata, have functioned as pressure-support strategies, but only within carefully monitored hydrodynamic limits to avoid triggering induced seismicity or compromising the long-term stability of the dual-reservoir system (Batini et al., 2003), (Santilano et al., 2016) (Fulignati et al., 2014), (Barelli et al., 2010), (Belgiorno et al., 2019). For Paipa–Iza, which currently lacks any installed infrastructure, this body of evidence indicates that reinjection design should not be deferred to a later operational phase, but treated as an early-stage engineering variable, linked from the outset to fracture-network connectivity and to a monitoring program capable of distinguishing natural from induced pressure and temperature changes (Alfaro et al., 2010), (Alfaro et al., 2020), (Nádor et al., 2020), (Szijártó et al., 2021).

Downhole and geophysical monitoring follows a parallel trajectory. The GMB and NGB analogues both demonstrate that distributed temperature and acoustic sensing (DTS/DAS), combined with 3D seismic and structural models, are what allow operators to quantify effective connectivity, anticipate cold-water breakthrough, and calibrate thermo-hydraulic models before committing to multi-well development (Wadas and von Hartmann, 2022), (Azzola and

Gaucher, 2024), (Schölderle et al., 2021), (Norden et al., 2023). Paipa–Iza's existing characterization already integrates magnetotellurics, gravimetry, and magnetometry to infer intrusive bodies and thermal anomalies (Norden et al., 2023), (Mantei et al., 2025); the comparative evidence from the GMB and NGB suggests that complementing this surface geophysical package with downhole instrumentation in future exploration wells is the logical next step to quantify fault connectivity and reduce drilling risk, rather than continuing to rely on surface data alone (Wadas and von Hartmann, 2022), (Agemar et al., 2018), (Azzola and Gaucher, 2024), (Bohnsack et al., 2021), (Schölderle et al., 2021).

Resource utilization strategy is the third recurring theme. The Pannonian Basin demonstrates that successful geothermal development at low-to-medium enthalpy does not require electricity generation: cascading uses — district heating, agro-industry, and balneology—allow systems to extract substantial value from moderate temperatures, while gradually expanding infrastructure as characterization and demand justify it (Toth and Nádor, n.d.), (Strasszer and Xydis, 2024). Given that Paipa–Iza's thermal regime (65–90°C) and current land use already carry a well-established balneological and tourism profile (Alfaro et al., 2010), (Alfaro-Valero et al., 2019) (Alfaro et al., 2020), this analogue is more directly transferable to Paipa–Iza's near-term development pathway than the high-enthalpy electricity-generation cases, and supports prioritizing direct-use and cascade-utilization schemes over premature assumptions about power generation potential (Toth and Nádor, n.d.), (Strasszer and Xydis, 2024).

Finally, the Tuscan analogues introduce an environmental dimension that is largely absent from the other comparisons but directly relevant given Paipa–Iza's magmatic component: Monte Amiata's documented water-table decline of 200–300 m in the central volcano, driven by depressurization propagating through vertically connected faults, together with the need for dedicated emissions management (H_2S, Hg) using technologies such as AMIS, demonstrates that systems with an igneous heat source and significant volatile content require environmental and hydrogeological baseline assessment from the earliest exploration stages, not as a retrofit once production begins (Bellani, 2018), (Mazzoldi et al., 2015), (Barelli et al., 2010), (Borgia et al., 2022). Given the volatile-rich crustal melting inferred for the Paipa Volcanic Complex (Alfaro et al., 2010), (Alfaro-Valero et al., 2019), (Gilbert, 2019), (Alfaro et al., 2020), this lesson is directly applicable to Paipa–Iza: a baseline of diffuse gas geochemistry and an assessment of deep-reservoir–aquifer connectivity should be established before any production decision is made (Belgiorno et al., 2019), (Borgia et al., 2022).

4.5 Integrated positioning of Paipa–Iza and future research priorities

Synthesizing the comparative evidence positions Paipa–Iza as a hybrid, early-stage system whose central uncertainties are not reducible to temperature alone, but concern where and how heat is generated, and where and how hydraulic connectivity is concentrated. Within the GMI framework (Table 6), Paipa–Iza's score of 0.3625 reflects this precisely: a system with already substantial technical characterization (0.75, driven by integrated geophysics, geochemistry, and structural analysis)(Alfaro et al., 2010), (Alfaro et al., 2020), (Gomez Romero, 2019), (González-Idárraga, 2021), but with no installed infrastructure and only an early-stage project status, placing it closer to Aachen (0.525)—another structurally promising but pre-infrastructure system (Gomez-Diaz et al., 2025), (Jüstel et al., 2022), (Gómez Díaz et al., 2024).

This positioning translates into three concrete priorities for advancing Paipa–Iza beyond its current maturity level. First, 3D structural and geophysical imaging—integrating 3D seismic where feasible with the existing magnetotelluric and gravimetric framework—is needed to resolve whether connectivity is dominated by faults, by discontinuities and karst-like features, or by stratigraphic facies, following the diagnostic logic established at Cerro Prieto, the GMB, and the NGB respectively (Lippmann et al., 1999), (Glowacka et al., 2005), (Wadas and von Hartmann, 2022), (Schölderle et al., 2021), (Norden et al., 2023), (González-Idárraga, 2021). Second, reservoir–seal architecture must be verified directly, since the Cerro Prieto and Tuscan analogues both show that seal continuity and leakage potential govern recharge and the long-term hydraulic response to drilling and production (Lippmann et al., 1999), (Glowacka et al., 2005), (Taussi et al., 2023), (Della Vedova et al., 2008). Third, a downhole monitoring program—distributed temperature and acoustic sensing, injection testing—should accompany any future drilling campaign to quantify connectivity empirically rather than inferring it solely from surface geophysics, mirroring practice at the GMB and NGB (Wadas and von Hartmann, 2022), (Azzola and Gaucher, 2024), (Schölderle et al., 2021), (Norden et al., 2023), (Mantei et al., 2025).

Beyond these immediate priorities, the comparative analysis identifies four research lines with direct relevance to Paipa–Iza's longer-term development: (i) quantitatively separating the magmatic and radiogenic contributions to the system's thermal budget through integrated petrophysical, geochemical, and geophysical analysis (Gomez Romero, 2019); (ii) constructing thermo-hydraulic numerical models that explicitly incorporate structural and stratigraphic heterogeneity, rather than simplified homogeneous assumptions, and testing their sensitivity to candidate reinjection scenarios (Mantei et al., 2025); (iii) developing a reinjection risk framework—covering clogging, scaling, and fluid–rock compatibility—informed by the documented experience in Hungary and Germany (Schölderle et al., 2021), (Bálint and Szanyi, 2015), (Markó et al., 2021); and (iv) incorporating hydrogeological-impact and gas-emissions assessment from the earliest project stages, following the lessons of Monte Amiata (Belgiorno et al., 2019), (Borgia et al., 2022). Collectively, these priorities reframe Paipa–Iza not merely as a geological prospect to be characterized, but as a socio-technical system in which exploration, engineering design, and sustainability considerations must co-evolve with the resource's most plausible near-term end use—thermal cascading, district heating, and thermal tourism (Strasszer and Xydis, 2024), (Batini et al., 2003), (Chiocchini et al., 2010).

4.6 Limitations

Despite the value of analogue transfer and the GMI framework, several limitations condition the interpretation presented above. First, the comparative dataset is constrained by uneven data availability and heterogeneity across analogue fields, so some dimensions—permeability architecture, reinjection performance, or monitoring intensity—are not documented with the same resolution in every case, which can bias cross-case pattern recognition. Second, the GMI is a simplified composite indicator: discretized classes, normalized scoring, and additive aggregation with equal weighting improve transparency and stability, but cannot capture site-specific thermodynamic, economic, or reservoir-engineering constraints, nor replace detailed field-specific evaluations. Third, for Paipa–Iza specifically, the central uncertainties identified throughout this discussion—heat-source partitioning between intrusions and possible radiogenic contributions, and the spatial distribution of effective hydraulic connectivity—remain non-unique without deep drilling and dedicated downhole

testing. Analogue-based inferences should therefore be treated as working hypotheses to be refined as new subsurface data become available, rather than as confirmed characterizations of the system.

The uncertainty ranges reported in this study are conditional on the scoring ladders, weighting distribution, and evidence-confidence probabilities adopted in the analysis. They should therefore be interpreted as methodological uncertainty intervals rather than frequentist confidence intervals. The confidence levels assigned to the categorical scores were based on the availability and consistency of the reviewed evidence and should be further evaluated through independent scoring by multiple experts. Future applications of the GMI could incorporate formal expert elicitation, inter-rater agreement statistics, and partially non-compensatory aggregation rules. A future validation round could, for example, engage five to eight independent domain experts to re-score each GMI component from the same evidence base, with inter-rater agreement quantified via Krippendorff's alpha or the intraclass correlation coefficient (ICC), and residual disagreements resolved through a structured, Delphi-style consensus process.

A further limitation concerns the benchmark dataset introduced in Section 2.1.1 and applied in Section 3.9: because its technical-characterization dimension was proxied by the number of documented study categories rather than by the same narrative expert judgment used for Paipa–Iza and the six analogues, its GMI values are methodologically parallel to, but not strictly identical in derivation to, the case-study scores reported in Section 3. The two approaches nonetheless converge closely for Paipa–Iza (Section 3.9), which supports the robustness of the low-maturity classification but does not eliminate the need for a fully narrative, database-wide re-scoring in future work.

4.7 Convergent Validation via a Structured Knowledge-Gap Diagnostic

As a further, independent line of evidence complementing the quantitative benchmarking in Section 3.9, the authors conducted a structured knowledge-gap diagnostic of the Paipa–Iza system, synthesizing the bibliometric analysis (Section 2.1.1), the six-analogue comparison (Section 3), and Colombian Geological Survey (Servicio Geológico Colombiano, SGC) technical documentation into a single evaluation matrix organized around seven knowledge dimensions: regional geology and tectonics; subsurface geophysics; geochemistry and hydrogeology; conceptual and numerical modeling; exploration, drilling, and production; environmental monitoring and reinjection; and social management and technology transfer. Each dimension was rated as High, Medium, Low, or Very low based on the level of validated information available, and individual gaps were further classified as informational (absence of measured or published data), methodological (lack of techniques or models adapted to the local context), or technological (lack of instrumentation or in-country capacity). The diagnostic was reviewed jointly by the Geotermia project's technical team and specialists from the SGC to verify its consistency with empirical data and operational reality.

The resulting matrix rates regional geology and tectonics as High — consistent with the well-documented fault network and stratigraphy summarized in Section 3.1 — and both geochemistry/hydrogeology and social management/thermal use as Medium, reflecting available but spatially and temporally sparse spring geochemistry data and an established but technically unmonitored balneological use, respectively. Subsurface geophysics, conceptual/numerical modeling, and environmental monitoring/reinjection are each rated Low, while exploration, drilling, and production is rated Very low, since no exploratory well deeper than 1000 m has been drilled at Paipa–Iza. This independently constructed, dimension-by-dimension diagnostic converges closely with the bibliometric coverage gradient reported in Section 2.1.1 (geology 76.0% versus geophysics 39.3% and drilling/production 31.1% of the global literature), providing a second, structurally different line of evidence for the same conclusion: the principal barriers to advancing Paipa–Iza are not resource availability but the depth of subsurface geophysical characterization, the absence of a calibrated 3D conceptual model, and the lack of exploratory drilling — precisely the priorities already identified in Section 4.5.

Beyond dimension-level ratings, the diagnostic distinguishes three gap types that carry different implications for near-term planning: informational gaps (vertical temperature profiles from shallow drilling, long-term time series of thermal-spring temperature, flow, and chemistry, and high-resolution integrated magnetotelluric–gravimetric–resistivity mapping), methodological gaps (the absence of a validated 3D conceptual model integrating geology, geophysics, and geochemistry, and of standardized monitoring and reinjection protocols for low-enthalpy systems), and technological gaps (limited in-field thermal instrumentation, the absence of locally calibrated reservoir-simulation software, and limited national technical capacity in multidisciplinary geothermal modeling). This typology reinforces the conclusion, developed independently in Sections 4.2–4.5, that the central challenge for Paipa–Iza is not geological unfavorability but the fragmentation of existing technical knowledge and the absence of multidisciplinary integration.

5. Conclusions

- The Paipa-Iza resource is defined as a low-to-medium enthalpy (65–90°C) hybrid geothermal system. Unlike purely sedimentary or magmatic systems, its potential results from magmatic anomalies induced by felsic intrusions, combined with a secondary radiogenic contribution from U-Th-K enrichment, and convection strongly controlled by structural connectivity.
- Geothermal viability in this system is governed by effective permeability along structural discontinuities—such as fault damage zones, fractures, and karstification—rather than primary matrix permeability. The hierarchical fault network and the Une Formation act as the main fluid conduits, replicating critical structural controls observed in mature analogues like Cerro Prieto and Tuscany.
- The implementation of the GMI demonstrates that geothermal maturity is not exclusively dictated by resource temperature, but rather by the comprehensive progress from exploration to commercial operation, including installed infrastructure and the level of technical characterization. Beyond this case study, the GMI is proposed as a reusable, transparent benchmarking layer for other early-stage hybrid and sedimentary-hosted geothermal systems in the Andes and elsewhere, complementing rather than replacing existing staged classification frameworks such as UNFC and GEA.
- To mitigate risk in future phases of Paipa-Iza, it is imperative to transcend surface exploration and implement 3D seismic inversion models alongside downhole monitoring (DTS/DAS systems) to quantify structural connectivity. Furthermore, given the projected focus on direct-use applications, the

design of reinjection schemes must be conceived as an early-stage engineering variable rather than a late adaptation, ensuring long-term pressure support and thermal sustainability.

Declarations

Acknowledgments

Acknowledgments: The authors thank Fundación Universidad de América for institutional support throughout the development of this research. The authors also acknowledge Universidad Agraria de Colombia (UNIAGRARIA) and Meridian Consulting, project partners in the "Evaluación integral del potencial geotérmico del complejo Paipa-Iza desde un estudio multidisciplinar" initiative, for their collaboration. Finally, the authors gratefully acknowledge the Ministerio de Ciencia, Tecnología e Innovación de Colombia (Minciencias) and the Agencia Nacional de Hidrocarburos (ANH) for their support of this project under Convocatoria 951 of 2024, Contract No. 061 of 2025.

Statements and Declarations

Funding: This research was funded by the Ministerio de Ciencia, Tecnología e Innovación de Colombia (Minciencias) in agreement with the Agencia Nacional de Hidrocarburos (ANH), under Call (Convocatoria) 951 of 2024, Contract No. 061 of 2025, as part of the project "Evaluación integral del potencial geotérmico del complejo Paipa-Iza desde un estudio multidisciplinar."

Competing interests: The authors declare no conflicts of interest.

Ethics approval: Not applicable

Consent to participate and consent for publication: Not applicable

Data, materials and/or code availability: No new primary data were generated in this study. All data supporting the reported results were derived from the previously published sources cited in the References section (particularly (Alfaro et al., 2010; Dijkshoorn et al., 2013; Alfaro-Valero et al., 2019; Gilbert, 2019; Beltrán, 2015; Alfaro et al., 2020; Gomez Romero, 2019; González-Idarraga, 2021) for the Paipa–Iza system, and the analogue-specific references cited throughout Section 3). The compiled comparative matrix and GMI scoring dataset generated for this analysis are available from the corresponding author upon reasonable request.

Author contributions: Conceptualization, A.S.-O.; methodology, A.S.-O. and A.P.; formal analysis, A.S.-O., D.A., H.A. and J.D.V.; investigation, D.A., H.A. and J.D.V.; data curation, D.A., H.A. and J.D.V.; writing—original draft preparation, A.S.-O.; writing—review and editing, A.S.-O. and A.P.; visualization, D.A., H.A. and J.D.V.; supervision, A.S.-O.; project administration, A.S.-O. All authors have read and agreed to the published version of the manuscript.

Abbreviations

$\delta^{18}O$	**Oxygen-18 isotopic composition**
$\delta^{2}H$	Hydrogen-2 isotopic composition
3D	Three-Dimensional
ATES	Aquifer Thermal Energy Storage
bar	bar (unit of pressure)
BTES	Borehole Thermal Energy Storage
°C	degree Celsius
°C/km	degrees Celsius per kilometer
Ca	Calcium
CPGF	Cerro Prieto Geothermal Field
CO2	Carbon Dioxide
DAS	Distributed Acoustic Sensing
DTS	Distributed Temperature Sensing
EGS	Enhanced Geothermal Systems
ERS	Elbe Reservoir Sandstone
ESP	Electric Submersible Pump
GMB	German Molasse Basin
GWth	Gigawatt thermal
Hg	Mercury
K	Potassium
K/km	Kelvin per kilometer
km	kilometer
H_2S	Hydrogen sulfide
HT-ATES	High-Temperature Aquifer Thermal Energy Storage
m	meter
m.a.s.l	Meters above sea level.
mD	millidarcy
Mg	Magnesium
mg/L	milligrams per liter
MPa	megapascal
MT	Magnetotelluric
mW/m^2	milliwatts per square meter
Mw	Moment Magnitude
MWth	Megawatt thermal
NGB	North German Basin
ORC	Organic Rankine Cycle
PIGS	Paipa – Iza Geothermal System.
PVC	Paipa Volcanic Complex
SGC	Colombian Geological Survey.
T/h	tonnes per hour
Th	Thorium
TWhth	Terawatt-hour thermal
U	Uranium

References

1. Ádám L, Cladouhos TT. (2016) Challenges of South Hungarian EGS Demonstration Project. https://www.researchgate.net/publication/309642993
2. Agemar T, Weber J, Moeck IS. (2018) Assessment and public reporting of geothermal resources in Germany: Review and outlook. Energies 11(2). https://doi.org/10.3390/en11020332
3. Aguilar A. (2006) Update of the Cerro Prieto Geological Model. GRC Trans 30.
4. Alfaro C, Velandia F, Cepeda H, Pardo N. Preliminary Conceptual Model of the Paipa Geothermal System. Colombia. Bali; 2010.
5. Alfaro C, Rueda J, Matiz C, Rodríguez G, González C, Beltrán M, Rodríguez G. and, Malo J. Updating of the Descriptive Conceptual Model of the Paipa Geothermal System. Colombia: In: GRC Transactions; 2020.
6. Alfaro-Valero C, Rueda-Gutiérrez J, Matiz C, Beltrán M, Rodríguez-Rodríguez G, Rodriguez-Ospina G, Gonzalez-Idarraga C, Malo J. Paipa Geothermal System, Boyacá: Review of Exploration Studies and Conceptual Model. Publicaciones Geológicas Especiales. 2019;161. https://doi.org/10.32685/pub.esp.38.2019.04.
7. Azzola J, Gaucher E. Seismic Monitoring of a Deep Geothermal Field in Munich (Germany) Using Borehole Distributed Acoustic Sensing. Sensors. 2024;24(10). https://doi.org/10.3390/s24103061.
8. Balcewicz M, Ahrens B, Lippert K, Saenger EH. Characterization of discontinuities in potential reservoir rocks for geothermal applications in the Rhine-Ruhr metropolitan area (Germany). Solid Earth. 2021;12(1):35–58. https://doi.org/10.5194/se-12-35-2021.
9. Bálint A, Szanyi J. A half century of reservoir property changes in the Szentes geothermal field, Hungary. Cent Eur Geol. 2015;58(1–2):28–49. https://doi.org/10.1556/24.58.2015.1-2.2.
10. Barelli A, Ceccarelli A, Dini I, Fiordelisi A, Giorgi N, Lovari F, Romagnoli P. A Review of the Mt. Amiata Geothermal System (Italy); 2010.
11. Batini F, Brogi A, Lazzarotto A, Liotta D, Pandeli E. Geological features of Larderello-Travale and Mt. Amiata geothermal areas (southern Tuscany, Italy). Enel GreenPower S.p.a. Via Andrea Pisano. - Pisa (Italy). 2003;26:120.
12. Beardsmore G, Ali A, Brommer M, Chen H, Conti P, Falcone G, Fridriksson T, Hogarth R, Mijnlieff H, Rumberg G, Ussher G. (2021) UNFC Resource Classification Applied to Real World Geothermal Projects: Outcomes from an Education and Implementation Pilot Program. In: Proceedings World Geothermal Congress 2020 + 1. Reykjavik.
13. Becker S, Hilgers C, Kukla PA, Urai JL. Crack-seal microstructure evolution in bi-mineralic quartz-chlorite veins in shales and siltstones from the RWTH-1 well, Aachen, Germany. J Struct Geol. 2011;33(4):676–89. https://doi.org/10.1016/j.jsg.2011.01.001.
14. Békési E, Fokker PA, Candela T, Szanyi J, van Wees JD. Ground motions induced by pore pressure changes at the Szentes geothermal area, SE Hungary. Geotherm Energy. 2022;10(1). https://doi.org/10.1186/s40517-022-00214-6.
15. Békési E, Van Wees JD, Porkoláb K, Hencz M, Berkesi M. Modelling the thermal evolution of extensional basins through lithosphere stretching factors: application to the NW part of the Pannonian Basin. Solid Earth. 2025;16(1):45–61. https://doi.org/10.5194/se-16-45-2025.
16. Belgiorno M, Sbrana A, Marianelli P, Baroni C. (2019) Natural CO2 degassing from the soil of Mt. Amiata volcanic-geothermal system. Pisa. https://tesidottorato.depositolegale.it/bitstream/20.500.14242/137623/1/PhD_thesis_Belgiorno.pdf
17. Bellani S, Brogi A, Lazzarotto A, Liotta D, Ranalli G. Heat flow, deep temperatures and extensional structures in the Larderello Geothermal Field (Italy): Constraints on geothermal fluid flow. J Volcanol Geoth Res. 2004;132(1):15–29. https://doi.org/10.1016/S0377-0273(03)00418-9.
18. Bellani S. Update of Heat Flow Data in the Geothermal Areas of Tuscany, Italy. Italy: Pisa; 2018.
19. Beltrán M. (2015) Ampliación del conocimiento geológico y del potencial de recursos del subsuelo de la nación investigación y exploración de recursos geotérmicos.
20. Bohnsack D, Potten M, Freitag S, Einsiedl F, Zosseder K. Stress sensitivity of porosity and permeability under varying hydrostatic stress conditions for different carbonate rock types of the geothermal Malm reservoir in Southern Germany. Geotherm Energy. 2021;9(1). https://doi.org/10.1186/s40517-021-00197-w.
21. Borgia A, Mazzoldi A, Micheli L, Grieco G, Calcara M, Balducci C. (2022) The Geothermal Power Plants of Amiata Volcano, Italy: Impacts on Freshwater Aquifers, Seismicity and Air. In: Progress in Volcanology. IntechOpen. https://doi.org/10.5772/intechopen.100558
22. Boyce AJ, Fulignati P, Sbrana A. Deep hydrothermal circulation in a granite intrusion beneath Larderello geothermal area (Italy): Constraints from mineralogy, fluid inclusions and stable isotopes. J Volcanol Geoth Res. 2003;126(3–4):243–62. https://doi.org/10.1016/S0377-0273(03)00150-1.
23. Castro CC (n.d.) Optimizing water reinjection in the Szentes Geothermal Field, editor. Hungary. https://www.researchgate.net/publication/391450752
24. Chiocchini U, Castaldi F, Barbieri M, Eulilli V. A stratigraphic and geophysical approach to studying the deepcirculating groundwater and thermal springs, and their recharge areas, in Cimini Mountains–Viterbo area, central Italy. Hydrogeol J. 2010;18(6):1319–41. https://doi.org/10.1007/s10040-010-0601-5.
25. Cozzini M. Guía de información para planificadores. Organización Latinoamericana de Energía (OLADE); 1994.
26. De Franco R, Petracchini L, Scrocca D, Caielli G, Montegrossi G, Santilano A, Manzella A. (2019) Synthetic Seismic Reflection Modelling in a Supercritical Geothermal System: An Image of the K-Horizon in the Larderello Field (Italy). Geofluids 2019. https://doi.org/10.1155/2019/8492453
27. De León Vivar J, De Dios Ocampo Diaz J, Pelayo A. (2001) New Tools for Reservoir Engineering in Cerro Prieto Geothermal Field. GRC Trans 25.
28. Della Vedova B, Vecellio C, Bellani S, Tinivella U. Thermal modelling of the Larderello geothermal field (Tuscany, Italy). Int J Earth Sci. 2008;97(2):317–32. https://doi.org/10.1007/s00531-007-0249-0.

29. Dijkshoorn L, Speer S, Pechnig R. (2013) Measurements and design calculations for a deep coaxial borehole heat exchanger in Aachen, Germany. International Journal of Geophysics 2013. http://dx.doi.org/10.1155/2013/916541
30. Elders WA, Williams AE, Biehler S. (1997) What Lies Beneath the Cerro Prieto Geothermal Field?.
31. Errázuriz-Henao C, Parolari M, Gómez-Tuena A, Gutiérrez-Aguilar F, García-Rodríguez H. Geochemical Evidence of Water-Fluxed Crustal Melting in the Northern Colombian Andes. J Petrol. 2024;65(7). https://doi.org/10.1093/petrology/egae073.
32. Fonseca H. (1982) The Cerro Prieto Geothermal Field: Geophysical Studies Conducted. https://library.geothermal.org/
33. Freitag S, Klaver J, Malai IS, Klitzsch N, Urai JL, Stollhofen H, Bauer W, Schmatz J. Petrophysical characterization, BIB-SEM imaging, and permeability models of tight carbonates from the Upper Jurassic (Malm ß), SE Germany. Geotherm Energy. 2022;10(1). https://doi.org/10.1186/s40517-022-00239-x.
34. Frondini F, Caliro S, Cardellini C, Chiodini G, Morgantini N. Carbon dioxide degassing and thermal energy release in the Monte Amiata volcanic-geothermal area (Italy). Appl Geochem. 2009;24(5):860–75. https://doi.org/10.1016/j.apgeochem.2009.01.010.
35. Fulignati P, Marianelli P, Sbrana A, Ciani V. 3D geothermal modelling of the mount amiata hydrothermal system in Italy. Energies. 2014;7(11):7434–53. https://doi.org/10.3390/en7117434.
36. Garofalo PS, Kiani F, Marchetti A, Lancellotti L, Vaselli O, Beccari S, Pedone G, Rappuoli D. Genesis of the hot spring mercury deposits of the Mt. Amiata geothermal system (Italy) constrained by Hg and S isotope geochemistry. Miner Deposita. 2026;61(1):147–62. https://doi.org/10.1007/s00126-025-01382-8.
37. Garrison GH, Guðlaugsson SÞ, Ádám L, Ingimundarson A, Cladouhos TT, Petty S. (2016) The South Hungary Enhanced Geothermal System (SHEGS) Demonstration Project.
38. Gilbert R-R. Interpolations from Vertical Electrical Soundings for the Characterization of the Geothermal System. Colombia: of the Municipality of Paipa; 2019.
39. Glowacka E, Sarychikhina O, Nava FA. Subsidence and stress change in the Cerro Prieto geothermal field. B C Mexico Pure Appl Geophys. 2005;162(11):2095–110. https://doi.org/10.1007/s00024-005-2706-7.
40. Gómez Díaz E, Wellmann F, Saar MO, Brehme M. (2024) Geothermal Reservoir Characterization of Paleozoic Limestones in the Northern Rhenish Massif. Rheinisch-Westfälischen Technischen Hochschule Aachen. https://publications.rwth-aachen.de/record/999977/files/999977.pdf
41. Gomez Romero DA, MODELO GEOTÉRMICO DE PAIPA MEDIANTE EXPLORACIÓN DEL SUBSUELO Y ANÁLISIS FÍSICO QUÍMICO DE AGUAS TERMALES. (2019). UNIVERSIDAD PEDAGÓGICA Y TECNOLÓGICA DE COLOMBIA, Tunja.
42. Gomez-Diaz E, Balza Morales A, Kukla P, Brehme M. Integrative analysis of the Aachen geothermal system (Germany) with an interdisciplinary conceptual model. Geotherm Energy. 2025. https://doi.org/10.1186/s40517-024-00327-0.
43. González-Idárraga CE. First Approach to 3D Resistive Model Interpretation in the Geothermal Area of Paipa, Colombia. In: GRC Transactions. Reykjavik; 2021.
44. Heldt S, Beyer C, Bauer S. Uncertainty assessment of thermal recovery and subsurface temperature changes induced by high-temperature aquifer thermal energy storage (HT-ATES): A case study. Geothermics. 2024;122. https://doi.org/10.1016/j.geothermics.2024.103086.
45. Helio M, Cfe R. (2000) Development History of Cerro Prieto (1973–2000). GRC Transactions 24.
46. Ilitch V, Federico G, Camacho Hernández JM. Principales Elementos del Play Geotérmico de Cerro Prieto, Baja California. XXX Congreso Anual. Morelia: Asociación Geotérmica Mexicana; 2024.
47. Invernizzi M, Scolieri GD, Tagliaferri F, Bettini A, Cinci M, Lenzi A, Sironi S. Dynamic Olfactometry Measurements of Geothermal Endogenous Gas Emissions. Chem Eng Trans. 2024;112:25–30. https://doi.org/10.3303/CET24112005.
48. Ito T, Ruiz C. Geothermal power: technology brief. International Renewable Energy Agency; 2017.
49. Izquierdo Montalvo G, Portugal E, Aragón A, Torres I, Alvarez J. (2001) Hydrothermal Mineralogy, Isotopy and Geochemistry in the Area of Cerro Prieto IV, Baja California Norte, Mexico. GRC Transactions 25.
50. Izquierdo Montalvo G, Aragón Aguilar A, Arellano VM, Rodriguez MH. (2010) Considerations on the Occurrence of Acid Fluids Formation in the Cerro Prieto IV Sector, México. GRC Transactions 34.
51. Jüstel A, Ritzmann O, Strozyk F, Kukla P. (2022) Interpretation of seismic reflection vintage lines from the Variscan Fold and Thrust Belt in the Aachen region, Germany: Implications for geothermal exploration. https://doi.org/10.5194/egusphere-egu22-9276
52. Koroncz P, Vizhányó Z, Farkas MP, Kuncz M, Ács P, Kocsis G, Mucsi P, Fedorné Szász A, Fedor F, Kovács J. (2022) Experimental Rock Characterisation of Upper Pannonian Sandstones from Szentes Geothermal Field, Hungary. Energies 15(23). https://doi.org/10.3390/en15239136
53. Krumbholz JF, Krumbholz M, Wadas SH, Tanner DC. Characterisation of the fracture- and karst-controlled geothermal reservoir below Munich from geophysical wireline and well information. Geotherm Energy. 2024;12(1). https://doi.org/10.1186/s40517-024-00286-6.
54. Lenkey L, Mihályka J, Paróczi P. Review of geothermal conditions of Hungary. Foldtani Kozlony. 2021;151(1):65–78. https://doi.org/10.23928/foldt.kozl.2021.151.1.65.
55. Liotta D, Bellani S, Brogi A, Manzella A, Ruggieri G, Zucchi M. The progress of geothermal knowledge at Larderello, Italy. Ital J Geosci. 2025;144(2). https://doi.org/10.3301/IJG.2025.05.
56. Lippmann M, Truesdell A, Fyre G. The Cerro Prieto and Salton Sea Geothermal fields-are they really alike? Twenty-Fourth Workshop on Geothermal Reservoir Engineering. Stanford: Stanford University; 1999.
57. Magi F, Vaselli O, Doveri M, Baroni C. (2016) Isotope geochemistry of rainfall, thermal and non-thermal waters from the Mt. Amiata area (northern-central Italy). Pisa. https://tesidottorato.depositolegale.it/bitstream/20.500.14242/137629/2/PhD_Thesis_MagiF_final_26042020.pdf

58. Magi F, Doveri M, Menichini M, Minissale A, Vaselli O. Groundwater response to local climate variability: hydrogeological and isotopic evidences from the Mt. Amiata volcanic aquifer (Tuscany, central Italy). Rend Lincei. 2019;30(1):125–36. https://doi.org/10.1007/s12210-019-00779-8.
59. Mantei N, Meneses Rioseco E, Moeck IS. Parametric analysis of geothermal reservoir performance in Mesozoic sandstone formations within the North German Basin developed by multi-well systems. Geotherm Energy. 2025;13(1). https://doi.org/10.1186/s40517-025-00349-2.
60. Markó Á, Mádl-Szőnyi J, Brehme M. Injection related issues of a doublet system in a sandstone aquifer - A generalized concept to understand and avoid problem sources in geothermal systems. Geothermics. 2021;97. https://doi.org/10.1016/j.geothermics.2021.102234.
61. Marroni M, Moratti G, Costantini A, Conticelli S, Benvenuti MG, Pandolfi L, Bonini M, Cornamusini G, Laurenzi MA. Geology of the Monte Amiata Region, Southern Tuscany, Central Italy. Ital J Geosci. 2015;134(2):171–99. https://doi.org/10.3301/IJG.2015.13.
62. Mazzoldi A, Borgia A, Ripepe M, Marchetti E, Ulivieri G, Schiava M, Allocca C. Faults strengthening and seismicity induced by geothermal exploitation on a spreading volcano, Mt. Amiata, Italia. J Volcanol Geoth Res. 2015;301:159–68. https://doi.org/10.1016/j.jvolgeores.2015.05.015.
63. Minissale A. (1991) The Larderello geothermal field: a review.
64. Moeck IS. Catalog of geothermal play types based on geologic controls. Renew Sustain Energy Rev. 2014;37:867–82. https://doi.org/10.1016/j.rser.2014.05.032.
65. Moeck I, Bracke R, Weber J. (2021) The Energy Transition from Fossil Fuels to Geothermal Energy-a German Case Study. In: Proceedings World Geothermal Congress. Reykjavik.
66. Morteani G, Voropaev A, Grinenko V. Relation of stibnite mineralisation and geothermal fluids in southern Tuscany (central Italy): An isotope (C, O, H, S) and Rare Earth Element study. Neues Jahrb Mineral Abh. 2017;194(3):279–96. https://doi.org/10.1127/njma/2017/0062.
67. Musumeci G, Bocini L, Corsi R. (2002) Alpine tectonothermal evolution of the Tuscan Metamorphic Complex in the Larderello geothermal field (northern Apennines, Italy). London. https://www.lyellcollection.org
68. Nádor A, Sebess-Zilahi L, Rotár-Szalkai Á, Gulyás Á, Markovic T. New methods of geothermal potential assessment in the Pannonian basin. Geologie en Mijnbouw/Netherlands J Geosci. 2020;98. https://doi.org/10.1017/njg.2019.7.
69. Njeru RM, Halisch M, Szanyi J. Micro-scale investigation of the pore network of sandstone in the Pannonian Basin to improve geothermal energy development. Geothermics. 2024;122. https://doi.org/10.1016/j.geothermics.2024.103071.
70. Norden B, Bauer K, Krawczyk CM. From pilot knowledge via integrated reservoir characterization to utilization perspectives of deep geothermal reservoirs: the 3D model of Groß Schönebeck (North German Basin). Geotherm Energy. 2023;11(1). https://doi.org/10.1186/s40517-022-00242-2.
71. Nur AAM, Nemes I, Bihari Z, Soltész H, Bárány Á, Tóth L, Borka S, Ferincz G. (2022) Naturally Fractured Carbonate Reservoir Characterization: A Case Study of a Mature High-Pour Point Oil Field in Hungary. In: SPWLA 63rd Annual Symposium Transactions. Society of Petrophysicists and Well Log Analysts. https://doi.org/10.30632/SPWLA-2022-0109
72. OECD. (2008) Handbook on Constructing Composite Indicators. Paris.
73. Olson E, Elders WA. (1978) Hydrothermal Mineralogy and Isotopic Geochemistry in the Cerro Prieto Geothermal Field, Mexico. II. Isotopic Geochemistry. GRC Transactions 2.
74. Open Energy Information (OpenEI). Geothermal Project Phases. U.S. Department of Energy; 2018. https://openei.org/wiki/Geothermal_Project_Phases.
75. Puente HG, Ribo-Muñoz M. Reinjection Experiences in the Cerro Prieto Geothermal Field. Geothermal Resources Council TRANSACTIONS 18; 1994.
76. Puente HG, Rodriguez MH. (1994) Cerro Prieto Steam Production Forecasting. GRC Transactions 18.
77. Puente I, De La Pena A, editors. (n.d.) Geología del Campo Geotérmico de Cerro Prieto.
78. Ros F, Ti S, Balsamo F, Villa IM, Ou MB, Bao U, E N N E Y. and, Faccenna C. (2008) Pliocene-Pleistocene HT-LP metamorphism during multiple granitic intrusions in the southern branch of the Larderello geothermal field (southern Tuscany, Italy). https://www.lyellcollection.org
79. Rosales JA. (2001) Geological Description and interpretation of Cores from Cerro Prieto Geothermal Field, Mexico. GRC Transactions 25.
80. Rueda-Gutiérrez JB. New evidences of magmatism in the Paipa geothermal system, Boyacá, Colombia. Bol de Geologia. 2020;42(3):51–79. https://doi.org/10.18273/revbol.v42n3-2020002.
81. Saccorotti G, Piccinini D, Zupo M, Mazzarini F, Chiarabba C, Agostinetti NP, Licciardi A, Bagagli M. The deep structure of the Larderello-Travale geothermal field (Italy) from integrated, passive seismic investigations. Energy Procedia. Elsevier Ltd; 2014. https://doi.org/10.1016/j.egypro.2014.10.371.
82. Santilano A, Godio A, Torino D, Russo S, Manzella A, Bruhn DF, Cardarelli E, Casas A, Girard F. (2016) Deep geothermal exploration by means of electromagnetic methods: New insights from the Larderello geothermal field (Italy). https://tesidottorato.depositolegale.it/bitstream/20.500.14242/166715/1/Santilano_thesis_PhD_2.pdf
83. Schölderle F, Lipus M, Pfrang D, Reinsch T, Haberer S, Einsiedl F, Zosseder K. Monitoring cold water injections for reservoir characterization using a permanent fiber optic installation in a geothermal production well in the Southern German Molasse Basin. Geotherm Energy. 2021;9(1). https://doi.org/10.1186/s40517-021-00204-0.
84. Shatyrbayeva I, Duschl F, Drews MC. (2024) Drilling data-calibrated shale compaction models for pore pressure evaluation from geophysical well logs in the North Alpine Foreland Basin, SE Germany. https://doi.org/10.6084/m9.figshare.c.7351073
85. Sindern S, Meyer FM, Lögering MJ, Kolb J, Vennemann T, Schwarzbauer J. Fluid evolution at the Variscan front in the vicinity of the Aachen thrust. Int J Earth Sci. 2011;101(1):87–108. https://doi.org/10.1007/s00531-011-0662-2.
86. Snyder H. Literature review as a research methodology: An overview and guidelines. J Bus Res. 2019;104:333–9. https://doi.org/10.1016/j.jbusres.2019.07.039.

87. Somma R, Granieri D, Troise C, Terranova C, De Natale G, Pedone M. Modelling of hydrogen sulfide dispersion from the geothermal power plants of Tuscany (Italy). Sci Total Environ. 2017;583:408–20. https://doi.org/10.1016/j.scitotenv.2017.01.084.
88. Strasszer D, Xydis G. Integrating geothermal energy in hungary: A case study on sustainable urban heating and emissions mitigation through the district heating infrastructure. Tunn Undergr Space Technol. 2024;149. https://doi.org/10.1016/j.tust.2024.105804.
89. Szanyi JD, Kovács B, Abdulhaq HA. (2026) Harnessing geothermal energy in Hungary. Geological Society, London, Special Publications 555(1). https://doi.org/10.1144/sp555-2024-22
90. Szijártó M, Galsa A, Tóth Á, Mádl-Szőnyi J. Numerical analysis of the potential for mixed thermal convection in the Buda Thermal Karst, Hungary. J Hydrology: Reg Stud. 2021;34. https://doi.org/10.1016/j.ejrh.2021.100783.
91. Szolga K, Árpád IW, Kocsis D. Municipal Geothermal Systems: Evaluation of Three Hungarian Cases. Int J Eng Manage Sci. 2024;9(2):81–93. https://doi.org/10.21791/ijems.2024.018.
92. Taussi M, Nisi B, Brogi A, Liotta D, Zucchi M, Venturi S, Cabassi J, Boschi G, Ciliberti M, Vaselli O. (2023) Deep Regional Fluid Pathways in an Extensional Setting: The Role of Transfer Zones in the Hot and Cold Degassing Areas of the Larderello Geothermal System (Northern Apennines, Italy). Geochemistry, Geophysics, Geosystems 24(6). https://doi.org/10.1029/2022GC010838
93. Toth AN. and Nádor A. (n.d.) Geothermal Country Update for Hungary. https://map.mbfsz.gov.hu/ogre_en/
94. Trumpy E, Gola G, Santilano A, Manzella A, Brambilla M, Calabrò R, Giussani M, Colombani RM, Palumbo S, Savoca V, Vajda E, Pisa. https://meetingorganizer.copernicus.org/EGU2020/presentation/EGU2020-21970
95. Vega-Ramírez LA, Contreras J, Fuentes-Bustillos K, Neumann F, Negrete-Aranda R, Spelz RM, Yarbuh I, Martín-Barajas A, González-Escobar M. (2025) Machine learning model of submarine heat flow in the thermally unexplored northern Gulf of California Rift System. Geothermics 132. https://doi.org/10.1016/j.geothermics.2025.103446
96. Volpi G, Magri F, Colucci F, Fisher T, De Caro M, Crosta GB. (2018) Modeling Highly Buoyant Flows in the Castel Giorgio: Torre Alfina Deep Geothermal Reservoir. Geofluids 2018. https://doi.org/10.1155/2018/3818629
97. Wadas SH, von Hartmann H. Porosity estimation of a geothermal carbonate reservoir in the German Molasse Basin based on seismic amplitude inversion. Geotherm Energy. 2022;10(1). https://doi.org/10.1186/s40517-022-00223-5.
98. Yin RK, Campbell DT. Case study research and applications: design and methods. SAGE Publications, Inc; 2018.

Figures

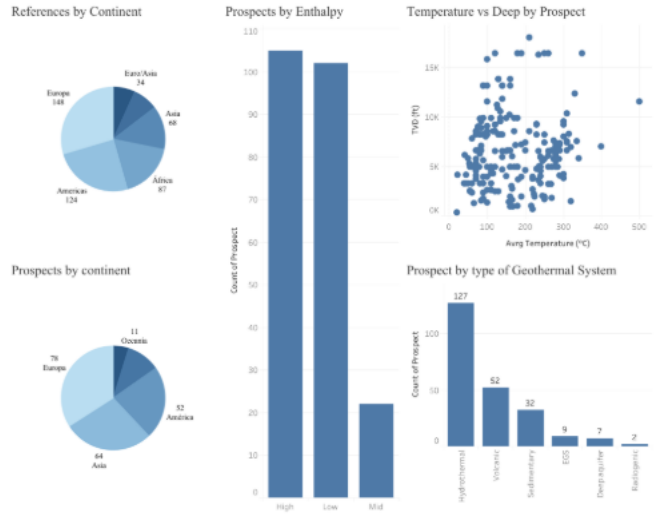


Figure 1

Summary of the global geothermal prospects analyzed in this study, including geographic distribution, enthalpy classification, geothermal system type, and reservoir temperature-versus-depth relationships.

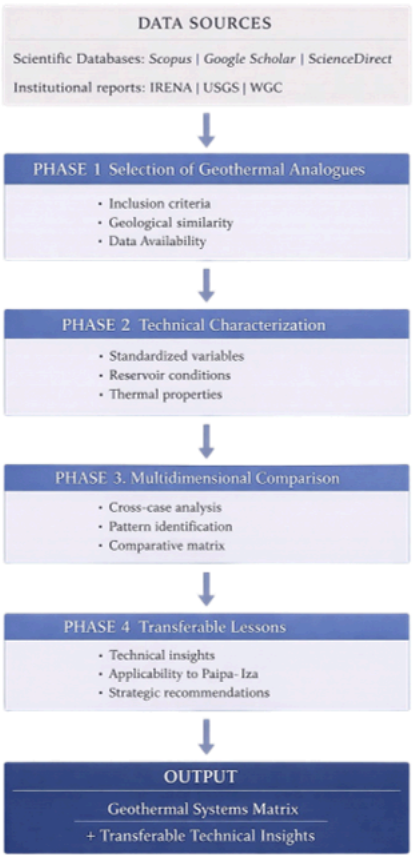


Figure 2

Methodological flowchart for the analogue-based comparative analysis applied to the Paipa–Iza Geothermal System.

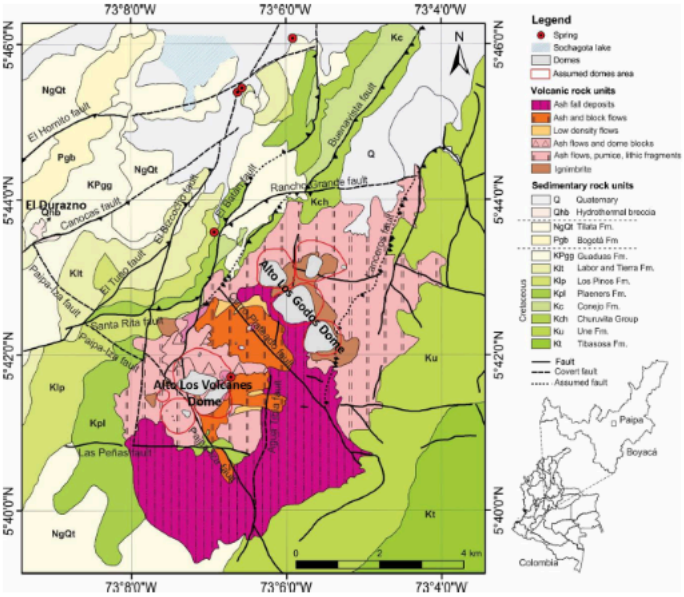


Figure 3

Location of the Paipa Geothermal System. Gonzalez – Idarraga. C.E. 2021. (p .2).

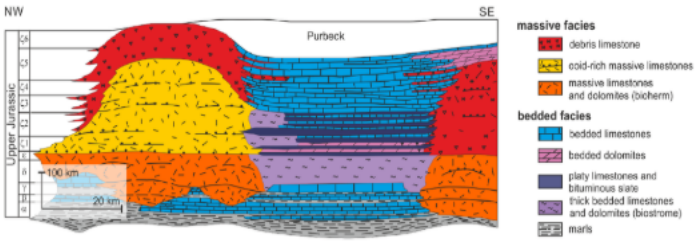


Figure 4

Conceptual facies characteristics and composition of the Upper Jurassic Malm strata below the Molasse Basin, separated into two hyper-facies: massive- and bedded-facies *(Krumbholz et al., 2024, p. 4).*

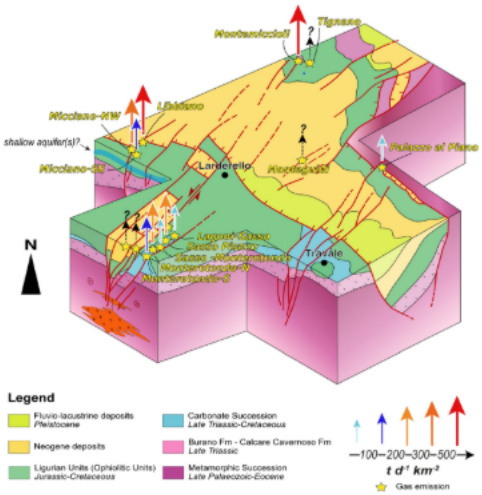


Figure 5

Geological sketch (not to scale) illustrating the tectonic context of the Larderello-Travale geothermal system. The main transfer zones and crustal faults that drive the occurrence of the main geothermal manifestation in the area are highlighted. The spatial distribution of the normalized endogenous CO2 diffuse emissions for the investigated sites is also reported (Taussi et al., 2023, p. 27).

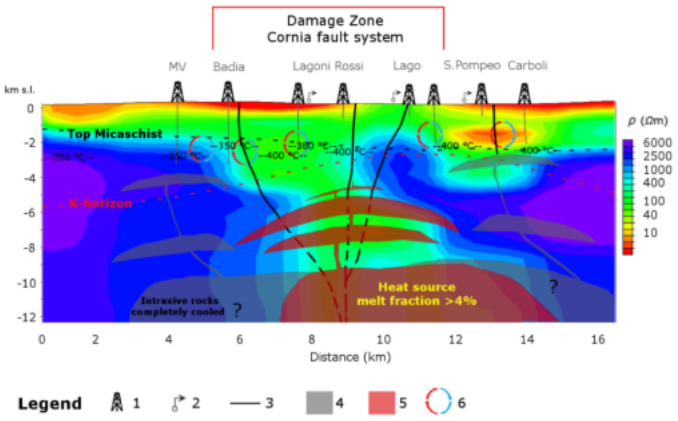


Figure 6

Conceptual model of the Lago Boracifero sector, based on the interpretation of the MT Profile1: **1)**productive wells in the proximity of the trace profile (max distance 800 m), **2)**main geothermal manifestation, **3)** main faults, **4)** supposed occurrence of completely cooled intrusion that cannot be imaged by resistivity anomaly, **5)** granitic intrusion with residual melt fraction higher than 4%, imaged by a wide resistivity anomaly, **6)** Active hydrothermal, vapor-dominated circulation and multi-stage hydrothermal alteration (Santilano et al., 2016, p. 202).

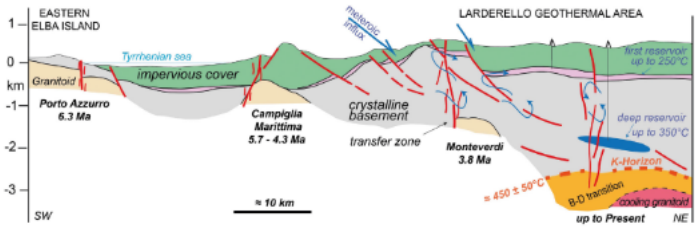


Figure 7

Structural sketch illustrating the present-day setting of the Larderello geothermal system within the context of eastward migration of magmatism, exhumation, uplift, and extensional tectonics. The latter is represented by normal and transfer faults that facilitate fluid circulation (after Dini et al., 2022, modified). Cooling ages are from: Spiess et al. (2021), Borsi et al. (1967), and Villa et al. (1987) (Liotta et al., 2025, p. 240).